MFN= 007376
01 SID/SCD
02 5997
03 INPE-5997-PRE/2112
04 MET
05 S
06 as
10 Obregon, Guillermo O.
10 Nobre, Carlos Afonso
12 Principal component analysis of precipitation fields over the Amazon river basin
14 35-46
30 Climanalise
31 5
32 7
40 Pt
41 Pt
41 En
42 <E>
58 CPTC
61 <PN>
64 jul. <1990>
68 PRE
76 ESTUDOS DO TEMPO E DO CLIMA
82 <BACIA AMAZONICA>
83 <abstract>Aplicou-se a Analise de Componentes Principais Rotacionadas (ACPR)as series temporais da precipitacao mensal de 28 estacoes pluviometricas da Bacia Amazonica com vistas a aumentar o entendimento de alguns dos padroes espaciais dos campos de precipitacao. As series de precipitacao cobrem o periodo de 35 anos (1951-1985). Efetuou-se ACPR para as series originais e, tambem, para series onde removeu-se o ciclo anual de modo a procurar-se os padroes de variabilidade inteanual dos campos de precipitacao. Os quatro primeiros Componentes Principais (CPs) explicam 65,1% (32,6%) da variancia para os casos com o ciclo (sem o ciclo) anual. Os dois primeiros padroes no caso com o ciclo anual relacionam-se fortemente a aspectos do ciclo sazonal de precipitacao na Amazonia: o dipolo norte-sul de maximas precipitacoes no hemisferio de verao para o primeiro padrao, e a migracao sazonal da ACIT (e linhas de instabilidade associadas na costa atlantica amazonica para o segundo padrao. A forma do primeiro padrao no sul da Amazonia segere uma associacao deste com o ciclo sazonal da Zona de Convergencia do Atlantico Sul (ZCAS). O segundo e quarto padroes do caso o sem ciclo annual parecem estar relacionados a eventos El Nino-Oscilacao Sul. Verificou-se esta associacao atraves da analise espectral cruzada entre o Indice de Oscilacao Sul e os coeficientes das series temporais (Scores) associados a estes padroes</abstract>
90 b
91 FDB-19961016
92 FDB-MLR

CONTRIBUIÇÕES REPRODUZIDAS NA ÍNTEGRA

PRINCIPAL COMPONENT ANALYSIS OF PRECIPITATION FIELDS OVER THE AMAZON RIVER BASIN

Guillermo O. Obregon and Carlos A. Nobre

Centro de Previsão de Tempo e Estudos Climáticos - CPTEC
Instituto de Pesquisas Espaciais-INPE
12201 São José dos Campos, SP, Brasil.

ABSTRACT

Rotated Principal Component Analysis (RPCA) was applied to time series of monthly precipitation for 28 stations of Amazon River Basin aiming at improving understanding of some of the spatial rainfall patterns. The precipitation series spanned 35 years(1951-1985). RPCA was performed for both the original series and also for the series which resulted after removal of the annual cycle from the original series. This was done in order to seek for patterns of interannual variability. The first four PC's explain 65.1 % (32.6 %) of total variance for the case with(without) the annual cycle. The first and second patterns of the case with the annual cycle are related to aspects of the seasonal cycle of precipitation over Amazonia: the north-south dipole of maximum precipitation in the summer hemisphere for the first pattern, and the ITCZ seasonal migrations (and related squall lines) along Amazonia's Atlantic Coast for the second. The shape of the first pattern in southern Amazonia suggests its association to the seasonal cycle of the South Atlantic Convergence Zone. The second and fourth patterns of the case without the annual cycle seem to be related to El Nino-South Oscillation (ENSO) events, which is corroborated by cross-spectrum analysis of the Southern Oscillation Index and the time series of the RPC Scores for those two patterns.

RESUMO

Aplicou-se a Análise de Componentes Principais Rotacionadas (ACPR) às séries temporais da precipitação mensal de 28 estações pluviométricas da Bacia Amazônica com vistas a aumentar o entendimento de alguns dos padrões espaciais dos campos de precipitação. As séries de precipitação cobrem o período de 35 anos (1951-1985). Efetuou-se ACPR para as séries originais e, também, para séries onde removeu-se o ciclo anual de modo a procurar-se os padrões de variabilidade interanual dos campos de precipitação. Os quatro primeiros Componentes Principais (CP's) explicam 65.1% (32.6 %) da variância para os casos com o ciclo (sem o ciclo) anual. Os dois primeiros padrões no caso com o ciclo anual relacionam-se fortemente à aspectos do ciclo sazonal de precipitação na Amazônia: o dipólo norte-sul de máximas precipitações no hemisfério de verão para o primeiro padrão, e a migração sazonal da ZCIT (e linhas de instabilidade associadas) na costa atlântica amazônica para o segundo padrão. A forma do primeiro padrão no sul da Amazônia segere uma associação deste com o ciclo sazonal da Zona de Convergência do Atlântico Sul (ZCAS). O segundo e quarto padrões do caso o sem ciclo annual parecem estar relarcionados a eventos El Nino-Oscilação Sul. Verificou-se esta associação através da análise espectral cruzada entre o Índice de Oscilação Sul e os coeficientes das séries temporais (Scores) associados a estes padrões.

1. INTRODUCTION

The region of study is located within latitudes 5°N and 19°S, and longitudes 45°W and 78°W, which approximately marks the limits of the Amazon Basin and lies within the tropical zone of South America. Spatial and temporal variability of rainfall (in this zone [3,8]) is large with strong seasonality. The nature of the precipitation distribution over the Amazon Basin has been investigated [15,19] and reviewed recently [17].

Traditionally, the rainfall climate of Amazonia has been mainly characterized by simple statistes based on monthly or annual totals [3,22]. Recently the climatological precipitation pattern was studied with the aid of EOF's [26]. In this study we used Rotated Principal Component Analysis (RPCA) to study the spatial and temporal variability of the monthly rainfall distribution in Amazonia.

2. DATA AND ANALYSIS METHODS

The data used in this study are the 35 year long (1951-1985) monthly rainfall records of 28 meteorological stations well distributed over the Amazon Basin, as shown in Figure 1. The time series lenght is 420 (35 years x 12 months) for each station. Additionally monthly values of the Southern Oscillation Index (SOI, mean monthly sea level pressure (SLP) anomaly at Darwin minus mean monthly SLP anomaly at Tahity) were used to construct a time series which was correlated to the time series of coefficients of the first 4 RPC's patterns of the precipitation distribution.

The basic principles of PCA are derived from the concept of dispersion of the inicial data matrix $Z(nxm)$; where $n = 420$ is the length of the monthly precipitation time series and $m = 28$ the number of stations. The analysis is performed in the space domain (S mode

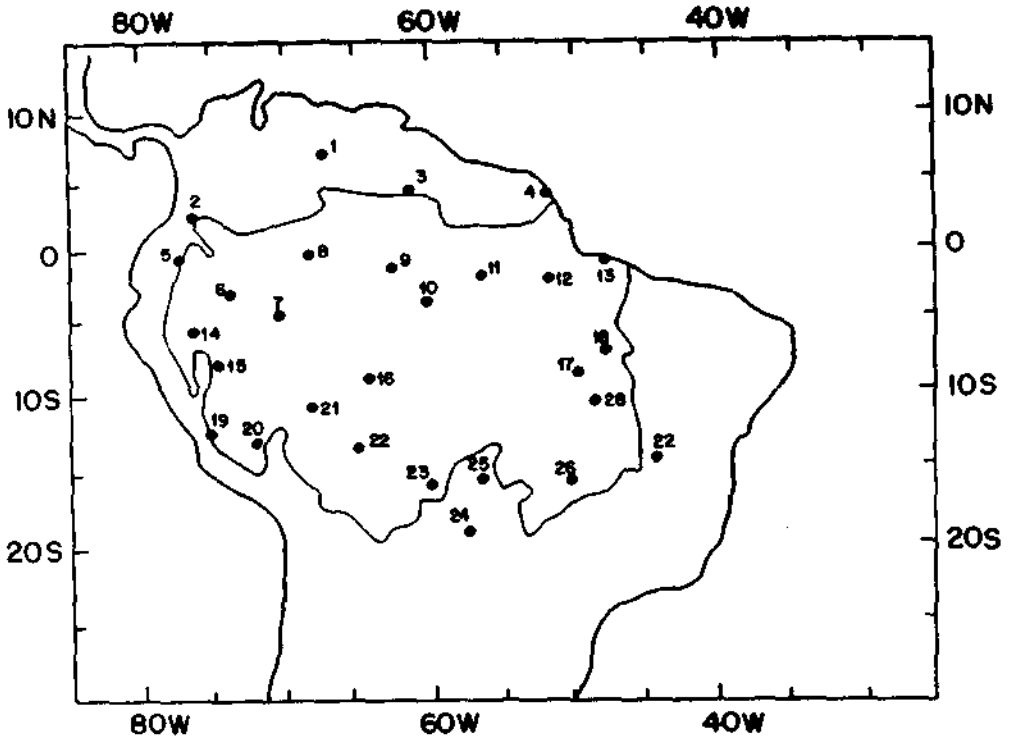

Fig. 1 - Study area and location of stations. The limits of the Amazon River Basin are indicated.

analysis) to describe the dominant spatial modes [25]. Thus the above PCA model takes the form of:

$$Z = FA^T$$

where: F(nxm) = Principal component scores
A(mxm) = Principal component loadings

Hence, the principal component loadings were obtained from the input of the correlation matrix R(28x28), which is justified by their advantages which include equal weighting of all the stations to avoid bias positioning of the "synoptic centres" [24].

Table 1 - The variances (eigenvalues) of the first six unrotated PCs of the precipitation field.

WITH SEASONAL CYCLE				WITHOUT SEASONAL CYCLE		
PC	VAR.	%	CUM.	VAR.	%	CUM.
1	2.0	42.5	42.5	3.3	11.8	11.8
2	3.6	12.9	55.4	2.2	7.8	19.6
3	1.6	5.5	60.9	1.9	6.9	26.5
4	1.2	4.2	65.1	1.7	6.1	32.6
5	1.0	2.9	68.0	1.4	5.1	37.7
6	0.8	2.6	70.6	1.3	4.6	42.3

The RPC analysis was done in two differents forms: i) with the unaltered time series, and ii)with a time series in which the annual cycle was removed by subtracting the 35-year mean precipitation for each month from the respective monthly value; thus two spatial matrices R(28x28) describing the inter-station correlation were generated. Each matrix was subjected to PCA in order to derive the PCs for these two cases. After obtaining the PCs, by the analysis of their Principal Components Loadings and the variance explained for each eigenvector, we rotated the first six Principal Components in the first case and eight in the second case through the Varimax Method in order to obtain a simple structure of the spatial patterns [25] and to improve their SACZ physical interpretation.

3. RESULTS OF THE ROTATED PRINCIPAL COMPONENT ANALYSIS

The variances (eigenvalues) obtained for both cases are shown in Table I.

In the first case the first four PC's explain 65.1 % of the precipitacion field total variance, whereas on the second case only 32.6 %. This fact can be attributed to the strong seasonal cycle, mainly represented by first PC, in the first case.

a) SERIES WITH SEASONAL CYCLE

In the distribution of the spatial pattern for the first case (Figures 2a-d), areas of maximum and minimum values are well delineated, and their associated time coefficients present strong seasonal cycle (Figures 3a-d); this strong seasonality can be clearly seen in the mean monthly values of the time coefficients (Figures 4a-d). The first spatial pattern (Fig. 2a) shows a marked minimum at the southwestern part of Amazonia with westward penetration; there is also a secondary minimum in the northwest and a maximum in the northern part. The time coefficient series of this pattern (Fig. 3a and 4a) shows positive values in northern summer and negative values in southern summer. This pattern is related to the very well-known dipole type precipitation regime over Amazonia with maximun (minimum) rainfall in the summer (winter) hemisphere. In the southern hemisphere summer the maximum rainfall area [8,22] is due to strong tropical convective activity [11,13,16] associated with the SACZ (South Atlantic Convergence Zone) and generated, in part, by equatorward advance of frontal systems which enhance convective activity [15,28]. Fig. 2b shows the second spatial pattern which presents a strong maximum in northeastern Amazonia over the Amazon river mouth, with a westward tongue-like penetration. The time coefficient series associated to this pattern appears to be related to the annual cycle of the rainfall which would be caused by the seasonal migration of the ITCZ over the Atlantic Ocean near the South American coast [9,27]. The ITCZ reachs its southern most latitude in March-April [27], which suggests that the second pattern may be related to it as the maximum of Fig. 4b occurs also in March-April. Additionally, this pattern appears to be associated to the squall lines [4,7] that form along the Atlantic Coast and propagate inland, where they gradually become less intense in general. The third spatial pattern (Fig. 2c) shows maximum values over the western part of Amazonia and over the Andes, and the time coefficient series (Fig. 3c and 4c) shows maximum values during April and Octobrer and minimum values during January and July. The coefficient series (Fig.3c) resembles the annual march of solar radiation at the Equador which is maximum during the equinoxes and minimun during the solstices. However, this pattern does not lend itself to simple interpretation. Finally the fourth spatial pattern (Fig. 2d) shows a dipole pattern with the Equator aproximately dividing the areas of positive and negative loadings. The time coefficient series (Fig. 3d and 4d) shows positive values in southern hemisphere summer and negative in the other seasons.

b) SERIES WITH ANNUAL CYCLE REMOVED

Figures 5a-d show the spatial patterns of the second case in which the annual cycle was removed. By removing the annual cycle we will be seeking for patterns of interannual variability of rainfall in Amazonia. The first and fourth spatial patterns show simpler structures. The first spatial pattern (Fig. 5a) is similar to the first one of the other case (Fig. 2a). This can be understood by calculating the correlation between the coefficients series for the two cases. The correlation coefficient is 0.65 which shows that the annual cycle was not completely removed and some seasonality still remained. The second spatial patterns (Fig. 5a) shows positive values in southwestern Amazonia and negative values over most of the region. The coefficient time series (Fig. 6b) seems to indicate that rainfall decreased during some ENSO events such as 57/58, 64/65 and 72/73. The third spatial pattern (Fig.5c) shows an area with minimum values in southern Amazonia. The fourth spatial pattern (Fig. 5d) is apparently associated to ENSO events since this spatial distribution agrees well with that of different studies which related ENSO events to precipitation anomalies in Amazonia [1,20]. The time coefficient series (Fig. 6d) shows an example of this relationship for 1982/1983 and 1957/1958.

In order to clarify our understanding of the relationship between ENSO events and the precipitation pattern over the Amazon basin we calculated linear correlations between the SOI time series and the coefficient series for the six RPC of the second case (Table II). In addition cross-spectrum analysis between the same time series was also done.

Table II - Correlation coefficients between the monthly SOI and the first six Rotated Principal Component Scores - RPCS.

RPCS	CORR. COEF.
1	0.08
2	-0.17**
3	-0.02
4	-0.24**
5	0.07
6	-0.09

** significant at 99% confidence level based on null hipotesis of zero correlation

The SOI time series and the coefficient series of the second and fourth pattern are statistically significant at 99% confidence level. Also the coherence-square between the second coefficient series and SOI (Fig.7) shows a peak between 2 and 3 years, statistically significant at 5 % level. This frequency range is one of the dominant frequencies of the ENSO phenomena [5] and it agrees with the frequency range found between the SOI and Amazon River discharges [23]. The coherence-square for the fourth coefficient series (Fig.8) shows a peak at 5 years and is statistically

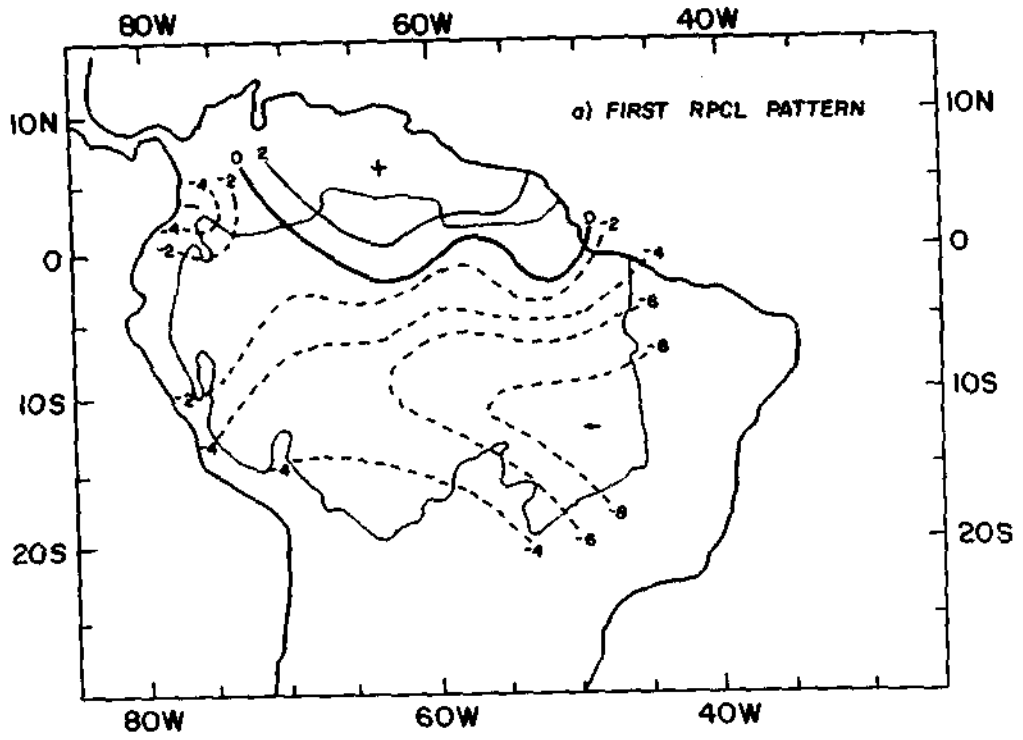

a) First RPCL pattern;

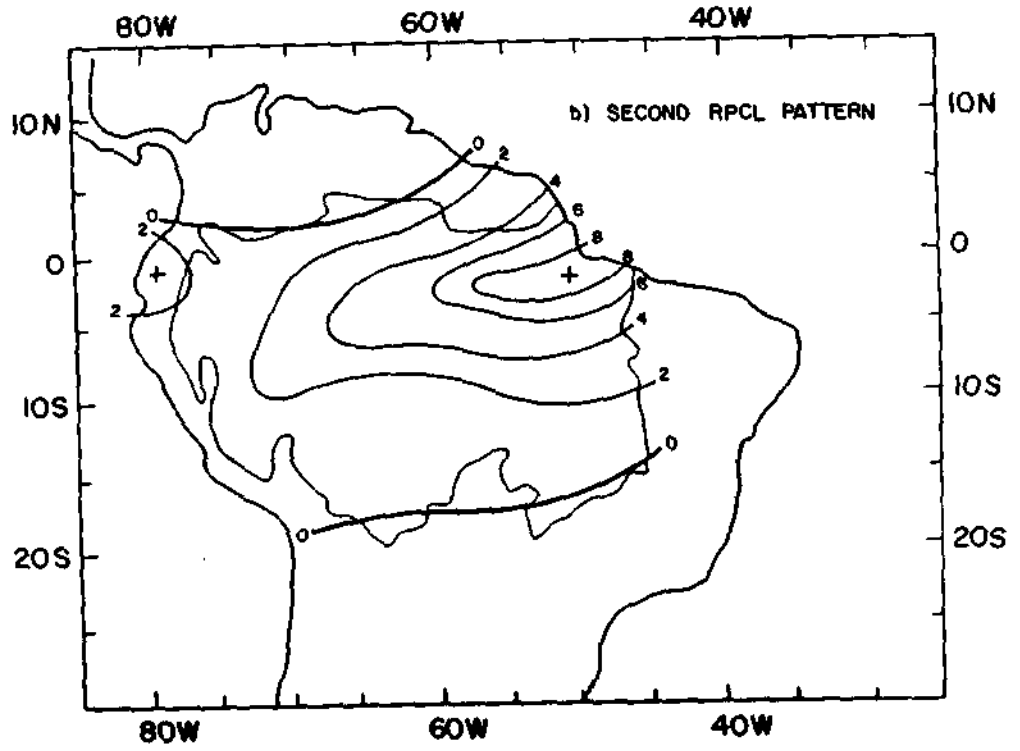

b) Second RPCL pattern;

Fig. 2 - Rotated Principal Component Loading contours (x10) of the first four RPC's of the precipitation field.

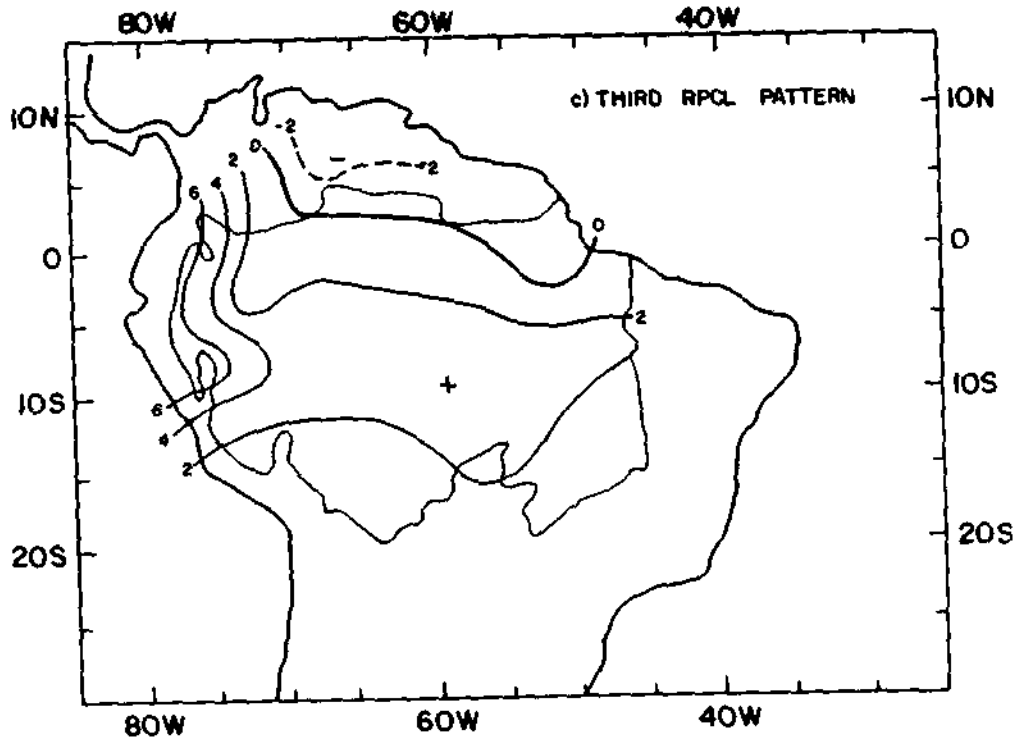

Fig. 2 - c) Third RPCL pattern;

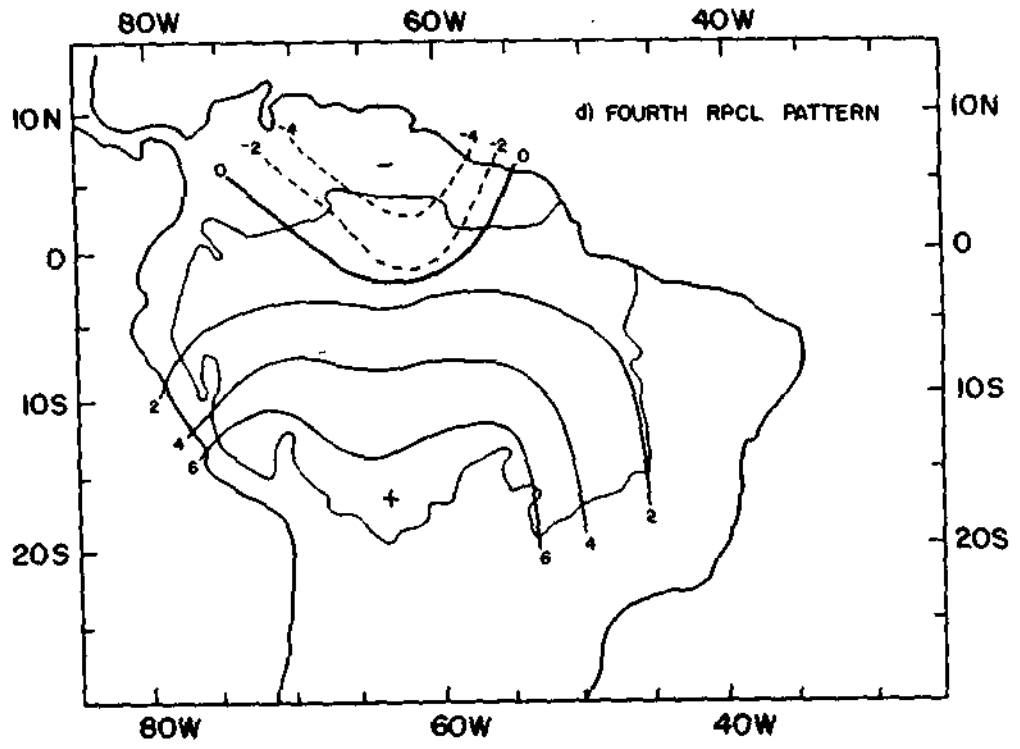

d) Fourth RPCL pattern;

FIG. 2 - Conclusão.

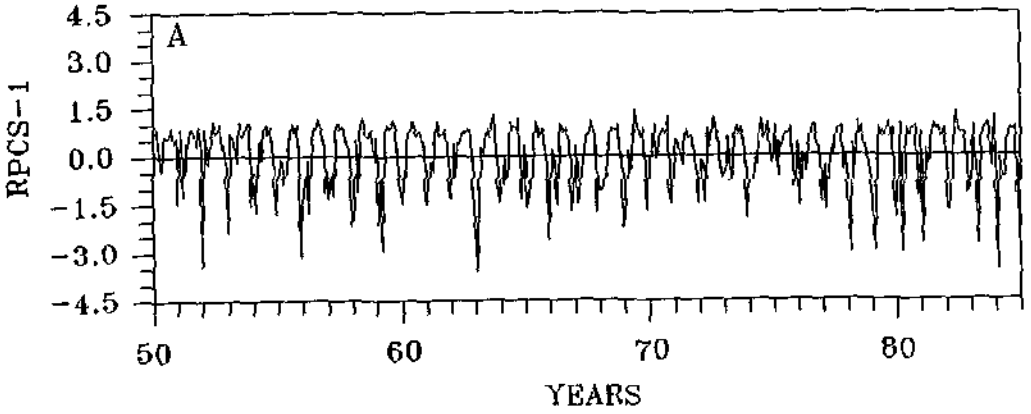

a) First RPCL pattern;

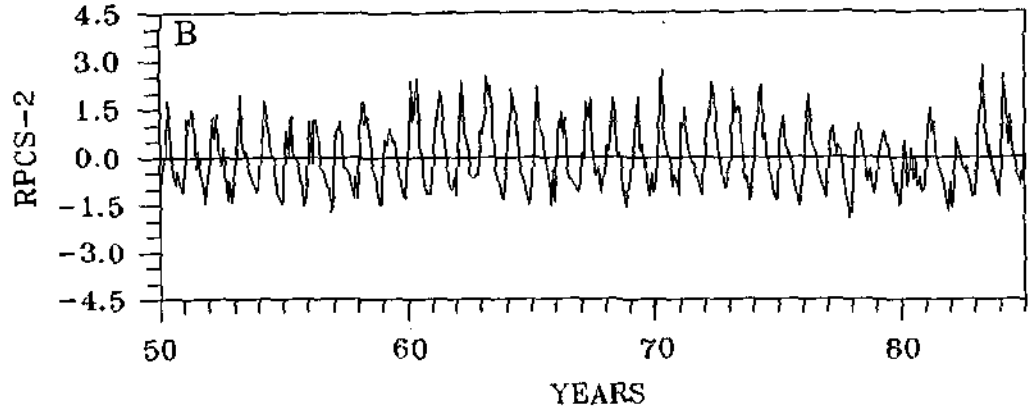

b) Second RPCL pattern;

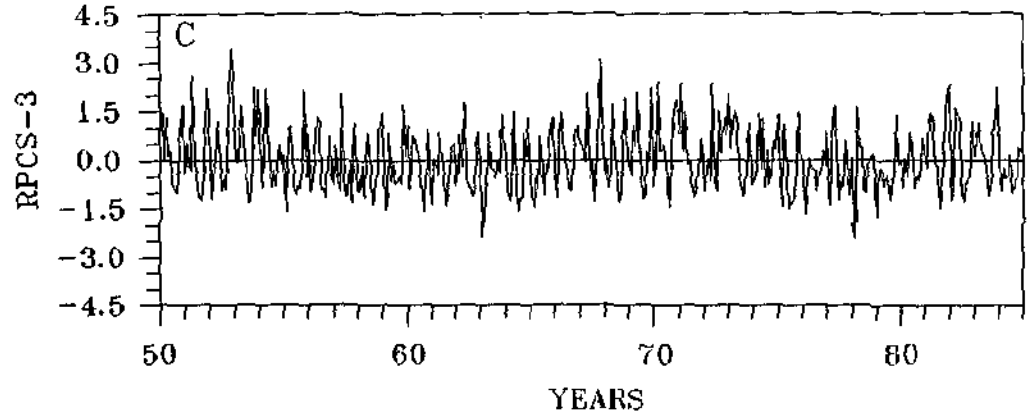

c) Third RPCL pattern.

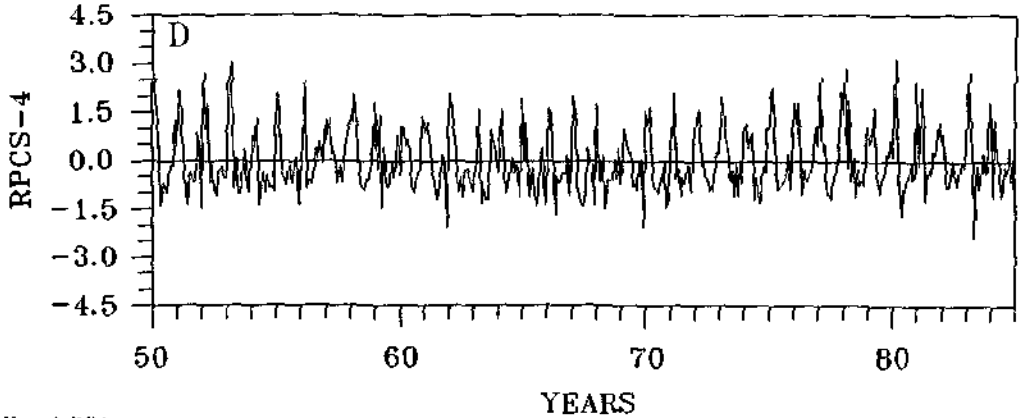

d) Fourth RPCL pattern;

Fig. 3 - RPC Scores of the first four RPC's of the precipitation fields

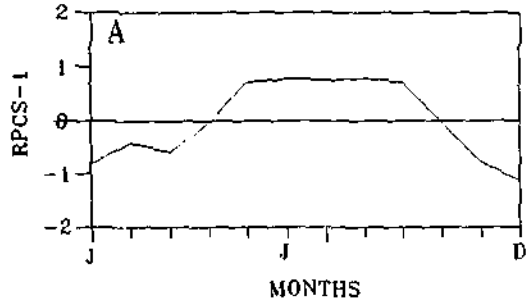

a) First RPCL pattern;

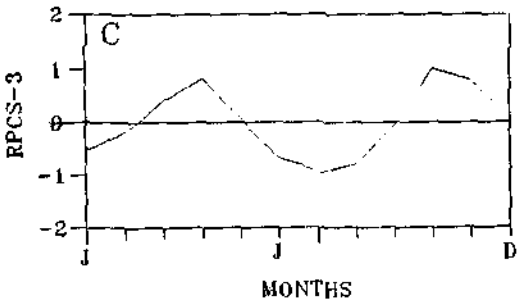

c) Third RPCL pattern;

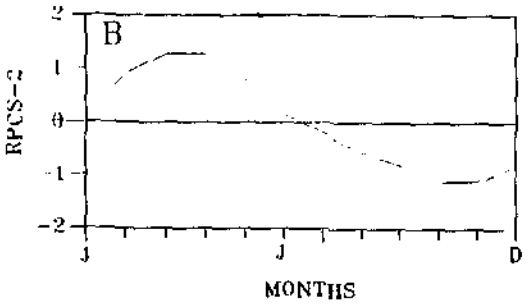

b) Second RPCL pattern;

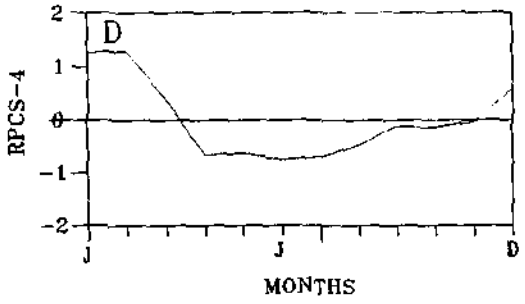

d) Fourth RPCL pattern;

Fig. 4 - As in Fig. 3 but for the Monthly mean score of of the first four RPCs of the precipitation field.

significant at 5% level. This spectral peak is also a dominant frequency observed for ENSO phenomena [5,6].

4. CONCLUSIONS

In this study, Rotated Principal Component Analysis (RPCA) was applied to time series of monthly precipitation for 28 stations in the Amazon River Basin. The aim of such analysis was to improve physical understanding of some of the rainfall patterns. The most important findings were the following:

1) With unaltered time series of precipitation (that is, series with annual cycle) two general conclusions can be drawn from the results of this case: i) The first pattern, which explains 42.5% of total variance, is associated with the strong dipole type climatological precipitation over Amazonia with maximum rainfall in the summer hemisphere and minimum rainfall in the winter hemisphere, showing mostly north-south precipitation gradients. The shape of this pattern in the southern Amazonia (NW-SE orientation) seems to indicate its relationship to the seasonal cycle of precipitation associated with the South Atlantic Convergence Zone [15,28]; ii) The second pattern explains 12.9% of total variance and is apparently related to the seasonal cycle of the ITCZ over the Atlantic Ocean and Amazonia's Atlantic Coast [9,18,27]; this pattern also appears to be associated with the squall lines which form along that coast [4,7]. The first two PC's explain 55.5 % of total variance and are strongly linked to the seasonal cycle of precipitation in Amazonia.

2) The annual cycle was removed from the time series to allow easier inspections of possible patterns of interannual variability in Amazonia. A relationship between ENSO events and rainfall over Amazonia seems to exist for the second and fourth patterns of this case. Correlation (Table II) and the cross-spectrum analysis between the SOI time series and the time coefficients series of the two patterns corroborate this finding.

The coefficient series of the second pattern, which is related to ENSO event in the frequency range of 2-3 year, seems to indicate that rainfall decreases during the ENSO events of 57/58, 64/65 and 72/73 but its spatial pattern does not possess a simple interpretation. The fourth pattern of this case, which is related to ENSO events in frequency range of 5 years, appears to be related to ENSO as other observational studies, also have found similar patterns for higher rainfall precipitation anomalies, that is, over northern Peru and Ecuador [10] and deficit precipitation over the eastern part of Amazonia [14,20], during ENSO episodes. This spatial patterns is also found in GCM experiment studies [2].

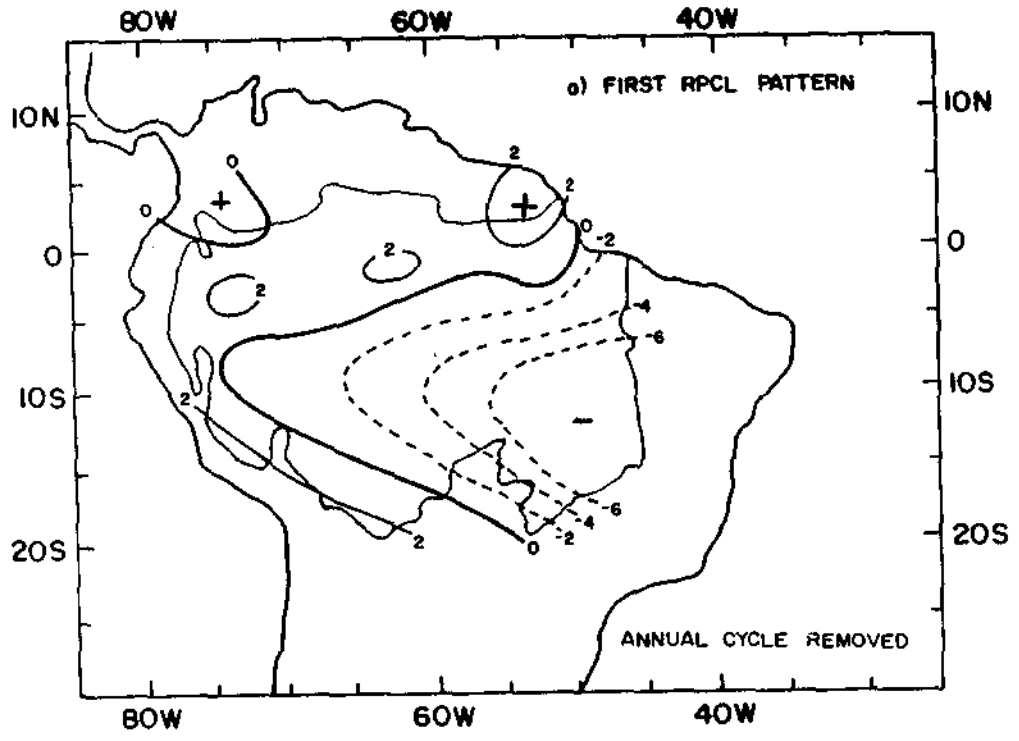

a) first RPCL pattern;

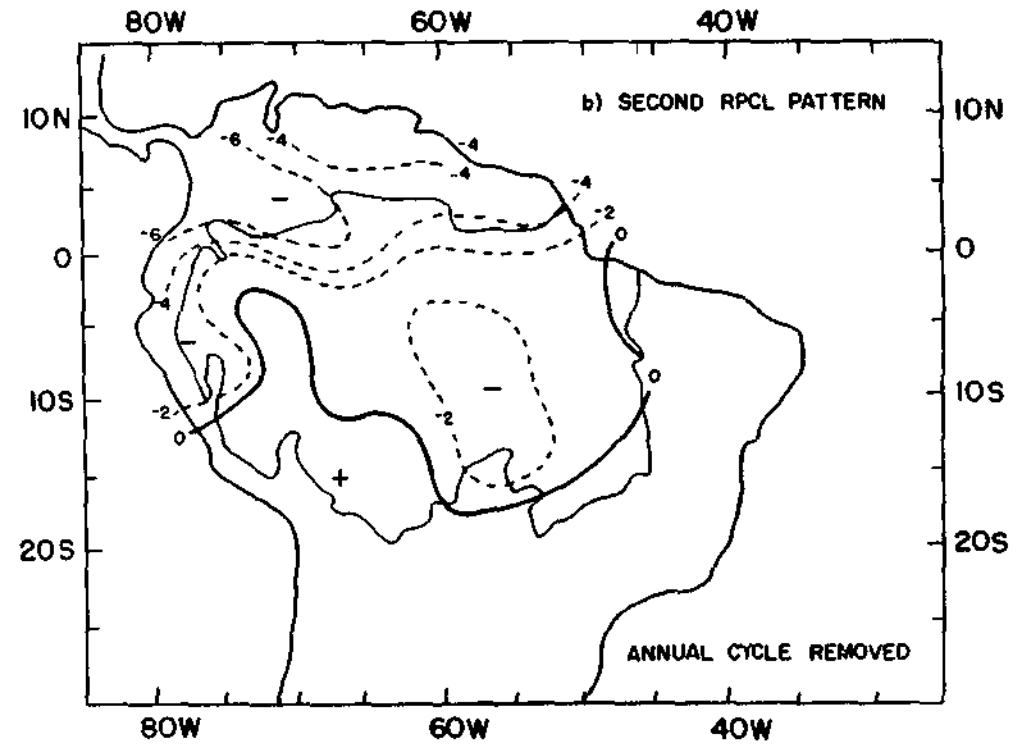

b) Second RPCL pattern;

Fig. 5 - As in Fig. 2 but for precipitation field without the annual cycle.

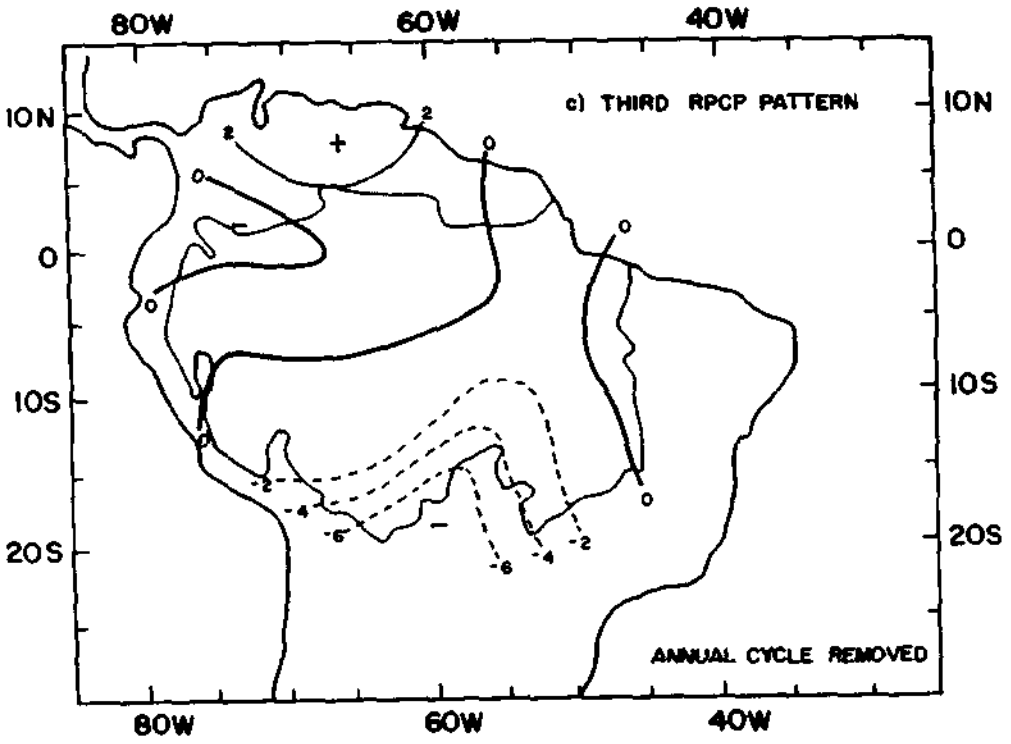

c) Third RPCL pattern;

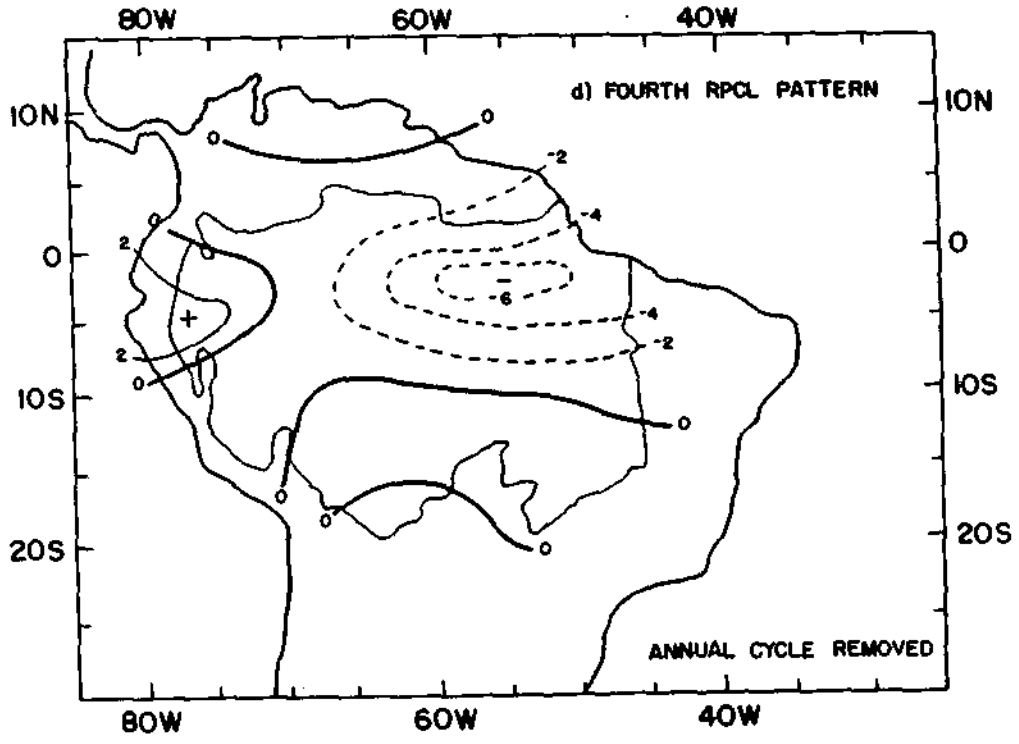

d) Fourth RPCL pattern;

Fig. 5 - Conclusão

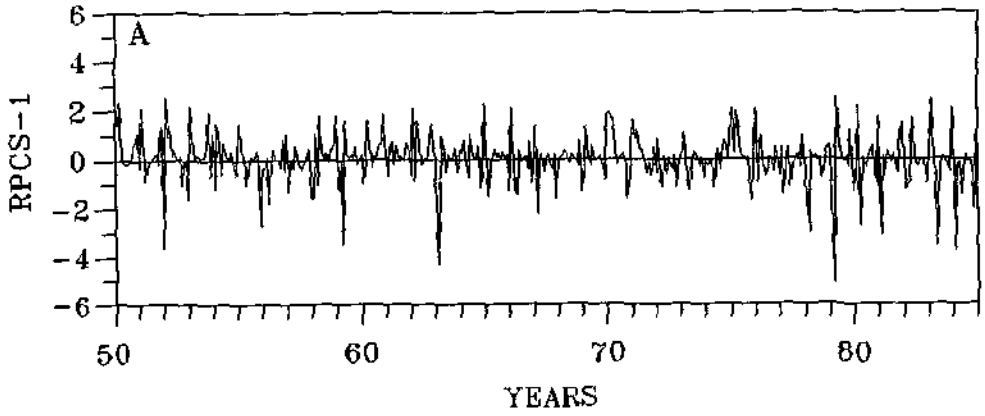

a) First RPCL pattern;

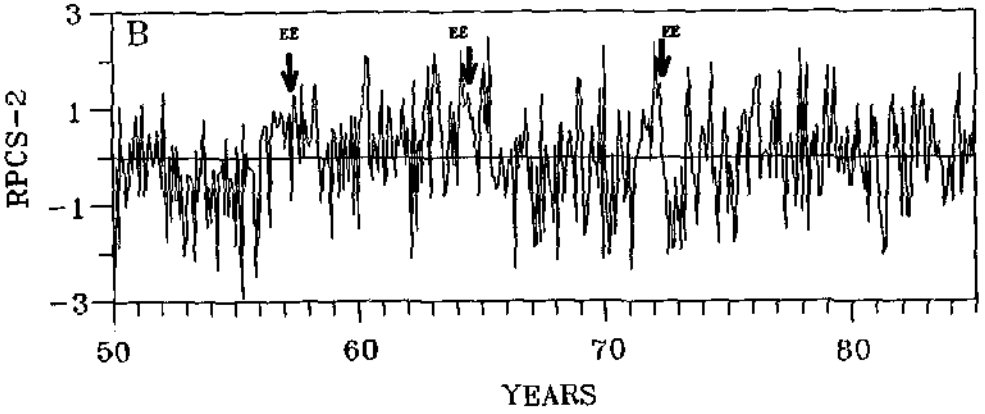

b) Second RPCL pattern;

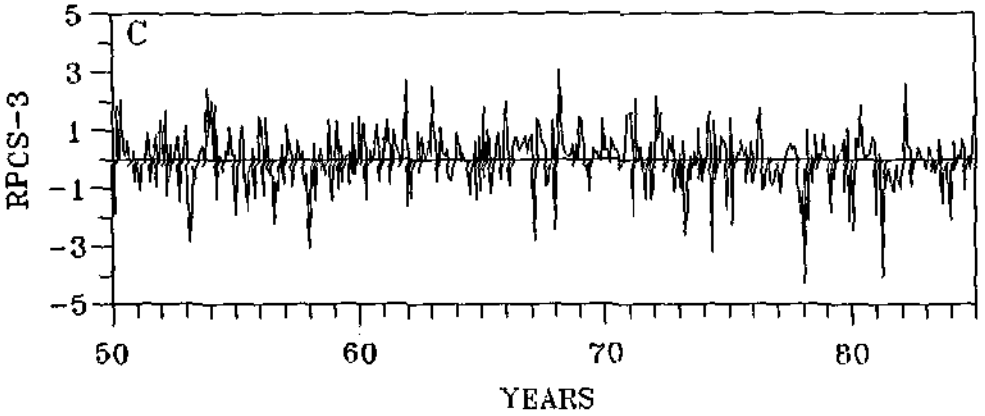

c) Third RPCL pattern;

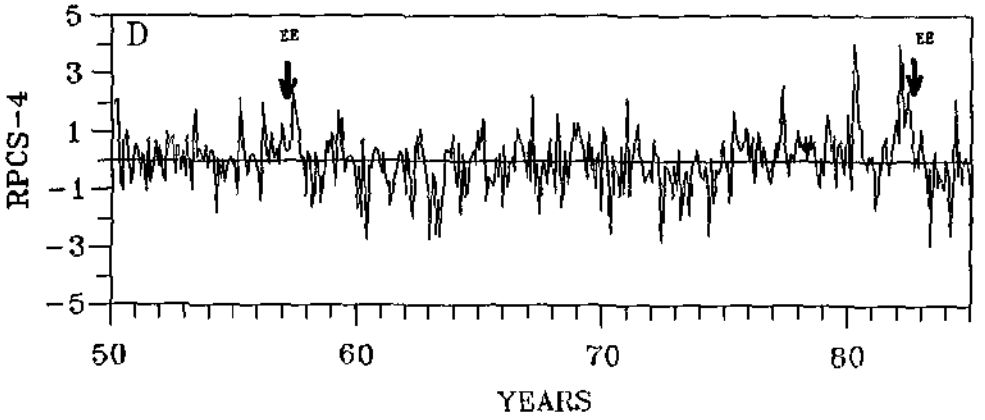

d) Fourth RPCL pattern;

Fig. 6 - As in Fig. 3 but for precipitation field without the annual cycle removed.

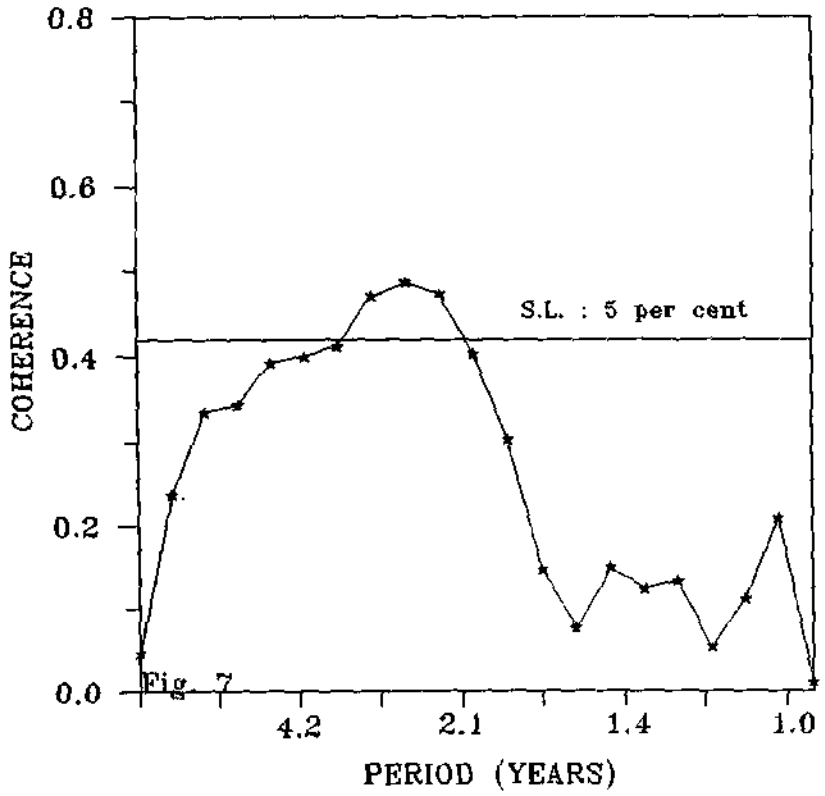

Figure 7 - Coherence square between Southern Oscillation Index (SOI) and RPC Scores of the second pattern without the annual cycle.

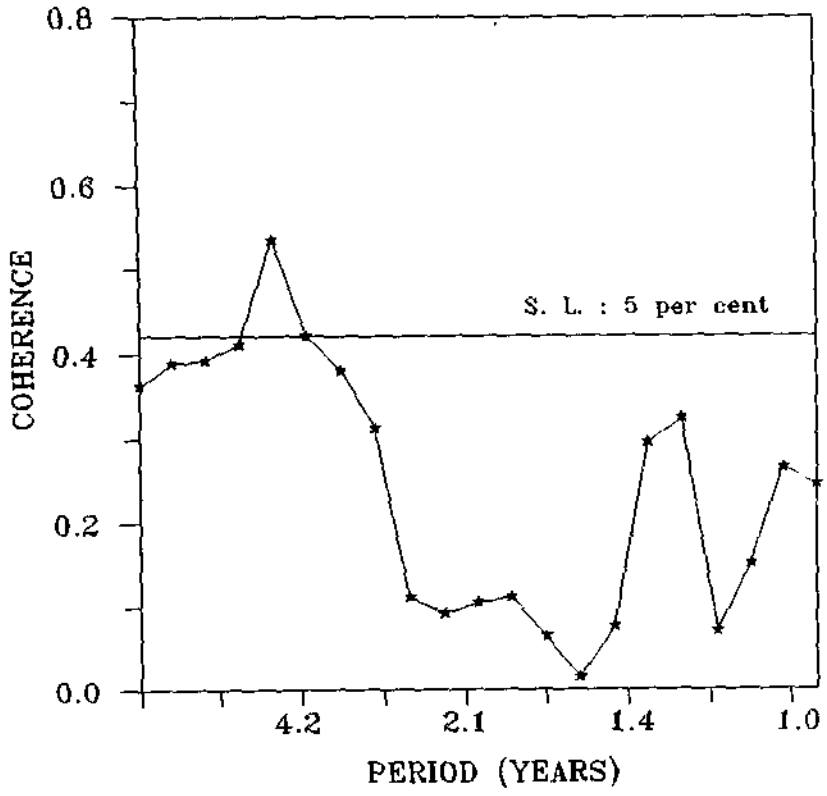

Figure 8 - As in Fig. 7 but for SOI and RPC Scores of the fourth pattern without the annual cycle.

5. ACKNOWLEDGEMENTS

We express our thanks to Paulo Nobre, Ana M. Gusmão and José Ivaldo B. de Brito for providing the corrected precipitation data set for Brazil, to José Marengo and Luis Caceres for providing part of rainfall data sets used in this study and to the Departamento Nacional de Águas e Energia Elétrica (DNAEE) of Brazil.

6. REFERENCES

[1] Aceituno, P., On the functioning of the Southern Oscillation in the South America sector, Mon. Wea.Rev. 116 (1988) 505-524.

[2] Buchman, J., Peagle, J., Buja, L. and Dickinson, R.E., Further FGGE forecast for Amazon Basin Rainfall, Mon.Wea. Rev. 117(1989) 1093-1102.

[3] Caviedes, C., Rainfall in South America, seasonal trends and spatial correlations, Erdkunde 35(1981) 107-118.

[4] Cavalcanti, I.F.A., Um estudo sobre interações entre sistemas de circulações de escala sinótica e circulações locais. Msc. Disertation, (INPE 2494-TDL/097) 1982.

[5] Chen, W.Y., Assessment of southern oscillation sea level pressure indices, Mon.Wea.Rev. 110(1982) 800-807.

[6] Chu, P.S. and Katz, R.W., Spectral estimation from time series models with relevance to Southern Oscillation, J.Climate. 2(1989) 86-90.

[7] Cohen, J.C., Da Silva Dias, M.A.F. and Nobre, C., Aspectos climatológicos das linhas de instabilidade na Amazônia, Climanálise, 4(11) 34-40. 1989.

[8] Figueroa, S.N. and Nobre, C.A., Precipitation distribution over central and western tropical South America, Climanálise, 5(6) 36-4, 1990.

[9] Hastenrath, S. and Heller, L., Dynamics of climatic hazards in Northeast Brazil, Quart.J.Roy Meteor.Soc. 35(1977) 77-92.

[10] Horel, J.D. and Cornejo-Garrido, A.G., Convection along the coast of Norhthern Peru during 1983: Spatial and temporal variation of cloud and rainfall, Mon.Wea.Rev 114(1986) 2091-2105.

[11] Horel, J.D., Hahmann, A.N. and Geisler, J.E., An investigation of convective activity over the Tropical Americas, J.Climate. 1(1989) 1388-1403.

[12] Kayano, M.T., Rao, V.B. and Moura,A.D., The Walker circulation and atmospheric water vapor characteristics over the Pacific for two contrasting years, J.Climatol. 9(1989) 243-252.

[13] Kousky, V.E. and Kagano, M.T., A climatological study of the tropospheric circulation over the Amazon Region, Acta Amazon. 11(1981) 743-758.

[14] Kousky, V.E., Kagano, M.T. and Cavalcanti, I.F.A., A review of the Southern Oscillation: Oceanic-atmospheric circulation changes and related rainfall anomalies, Tellus, 36 A(1984) 490-504.

[15] Kousky, V.E., Atmospheric circulation changes associated with rainfall anomalies over Tropical Brazil, Mon. Wea. Rev. 113 (1985) 1951-1957.

[16] Kousky, V.E., Pentad outgoing longwave radiation climatology for the South America sector, Rev. Bras. de Meteo. 3(1988) 217-231.

[17] Molion, L.C.B., Climatologia dinâmica da região Amazônica: mecanismos de precipição, Rev.Bras. de Metoro. 2(1987) 107-117.

[18] Moura, A.D. and Shukla, J., On the dynamics of droughts in Northeast Brazil: Observations, theory and numerical expriment with a general General Circulation Model, J. Atmos.Sci. 38(1981) 2653-2675.

[19] Nishizawa, T. and Tanaka, M., The annual changes in the tropospheric circulation and rainfall in South America, Arch.Met.Geoph.Biocl., Ser. B, 33(1983) 107-116.

[20] Nobre, C. and Rennó, N.D., Droughts and floods in South America due to the 1982-83 ENSO episode, in: Proceedings of the 6th Conference on Hurricanes and Tropical Meteorology, AMS., 14-17 May., Houston, Texas, (1985) 131-133.

[21] Oliveira, A.S., Interações entre sistemas frontais na América do Sul e convecção na Amazônia, Tese de Mestrado, INPE-4008-TDL/239, (1986).

[22] Ratisbona, L.R.,The climate of Brazil, in: W. Schwerdtfeger, (eds), Vol. 12, Climates of central and South America(Elsevier, Amsterdam, 1976).

[23] Richey, J.E., Nobre, C. and Deser, C. Amazon river discharge and climatic variability: 1903 to 1985, Science, 246(1989) 101-103.

[24] Richman, M.B., Obliqued rotated Principal Components, An improved meteorological map typing technique?, J.Appl.Meteorol. 20(1981) 1145-1159.

[25] Richman, M.B., Rotation of Principal Components, J.Climatol. 6(1986) 293-335.

[26] Santos, L. do Nacimento, A. and Da Silva, M.G., Um estudo da precipitação da região Amazônica Brasileira usando autovetores empíricos, in: Anais do V Congreso Brasileiro de Meteorologia, Rio de Janeiro (Janeiro 7-Novembro 11 1988).

[27] Uvo, C.R.B., Zona de Convergência intertropical(ZCIT) e sua relação com a precipitação da região Norte e Nordeste Brasil, MSc. Disertation., INPE 4887-TDL/378, (1989).

[28] Virji, H. and Kousky, V.E. Regional and global aspects of the low latitude frontal penetration in Amazonas and associated tropical activity, in: Preprints of the First International Conf. of Southrn Hemisphere Meteology, AMS, São José dos Campos-Brasil (July 31-August 6 1983).

CONTRIBUIÇÕES REPRODUZIDAS NA ÍNTEGRA

PRINCIPAL COMPONENT ANALYSIS OF PRECIPITATION FIELDS OVER THE AMAZON RIVER BASIN

Guillermo O. Obregon and Carlos A. Nobre

Centro de Previsão de Tempo e Estudos Climáticos - CPTEC.
Instituto de Pesquisas Espaciais-INPE
12201 São José dos Campos, SP, Brasil.

ABSTRACT

Rotated Principal Component Analysis (RPCA) was applied to time series of monthly precipitation for 28 stations of Amazon River Basin aiming at improving understanding of some of the spatial rainfall patterns. The precipitation series spanned 35 years(1951-1985). RPCA was performed for both the original series and also for the series which resulted after removal of the annual cycle from the original series. This was done in order to seek for patterns of interannual variability. The first four PC's explain 65.1 % (32.6 %) of total variance for the case with(without) the annual cycle. The first and second patterns of the case with the annual cycle are related to aspects of the seasonal cycle of precipitation over Amazonia: the north-south dipole of maximum precipitation in the summer hemisphere for the first pattern, and the ITCZ seasonal migrations (and related squall lines) along Amazonia's Atlantic Coast for the second. The shape of the first pattern in southern Amazonia suggests its association to the seasonal cycle of the South Atlantic Convergence Zone. The second and fourth patterns of the case without the annual cycle seem to be related to El Nino-South Oscillation (ENSO) events, which is corroborated by cross-spectrum analysis of the Southern Oscillation Index and the time series of the RPC Scores for those two patterns.

RESUMO

Aplicou-se a Análise de Componentes Principais Rotacionadas (ACPR) às séries temporais da precipitação mensal de 28 estações pluviométricas da Bacia Amazônica com vistas a aumentar o entendimento de alguns dos padrões espaciais dos campos de precipitação. As séries de precipitação cobrem o período de 35 anos (1951-1985). Efetuou-se ACPR para as séries originais e, também, para séries onde removeu-se o ciclo anual de modo a procurar-se os padrões de variabilidade interanual dos campos de precipitação. Os quatro primeiros Componentes Principais (CP's) explicam 65.1% (32.6 %) da variância para os casos com o ciclo (sem o ciclo) anual. Os dois primeiros padrões no caso com o ciclo anual relacionam-se fortemente à aspectos do ciclo sazonal de precipitação na Amazônia: o dipólo norte-sul de máximas precipitações no hemisfério de verão para o primeiro padrão, e a migração sazonal da ZCIT (e linhas de instabilidade associadas) na costa atlântica amazônica para o segundo padrão. A forma do primeiro padrão no sul da Amazônia segere uma associação deste com o ciclo sazonal da Zona de Convergência do Atlântico Sul (ZCAS). O segundo e quarto padrões do caso o sem ciclo annual parecem estar relarcionados a eventos El Nino-Oscilação Sul. Verificou-se esta associação através da análise espectral cruzada entre o Índice de Oscilação Sul e os coeficientes das séries temporais (Scores) associados a estes padrões.

1. INTRODUCTION

The region of study is located within latitudes 5°N and 19°S, and longitudes 45°W and 78°W, which approximately marks the limits of the Amazon Basin and lies within the tropical zone of South America. Spatial and temporal variability of rainfall (in this zone [3,8]) is large with strong seasonality. The nature of the precipitation distribution over the Amazon Basin has been investigated [15,19] and reviewed recently [17].

Traditionally, the rainfall climate of Amazonia has been mainly characterized by simple statistcs based on monthly or annual totals [3,22]. Recently the climatological precipitation pattern was studied with the aid of EOF's [26]. In this study we used Rotated Principal Component Analysis (RPCA) to study the spatial and temporal variability of the monthly rainfall distribution in Amazonia.

2. DATA AND ANALYSIS METHODS

The data used in this study are the 35 year long (1951-1985) monthly rainfall records of 28 meteorological stations well distributed over the Amazon Basin, as shown in Figure 1. The time series lenght is 420 (35 years x 12 months) for each station. Additionally monthly values of the Southern Oscillation Index (SOI, mean monthly sea level pressure (SLP) anomaly at Darwin minus mean monthly SLP anomaly at Tahity) were used to construct a time series which was correlated to the time series of coefficients of the first 4 RPC's patterns of the precipitation distribution.

The basic principles of PCA are derived from the concept of dispersion of the inicial data matrix Z(nxm); where n = 420 is the length of the monthly precipitation time series and m = 28 the number of stations. The analysis is performed in the space domain (S mode

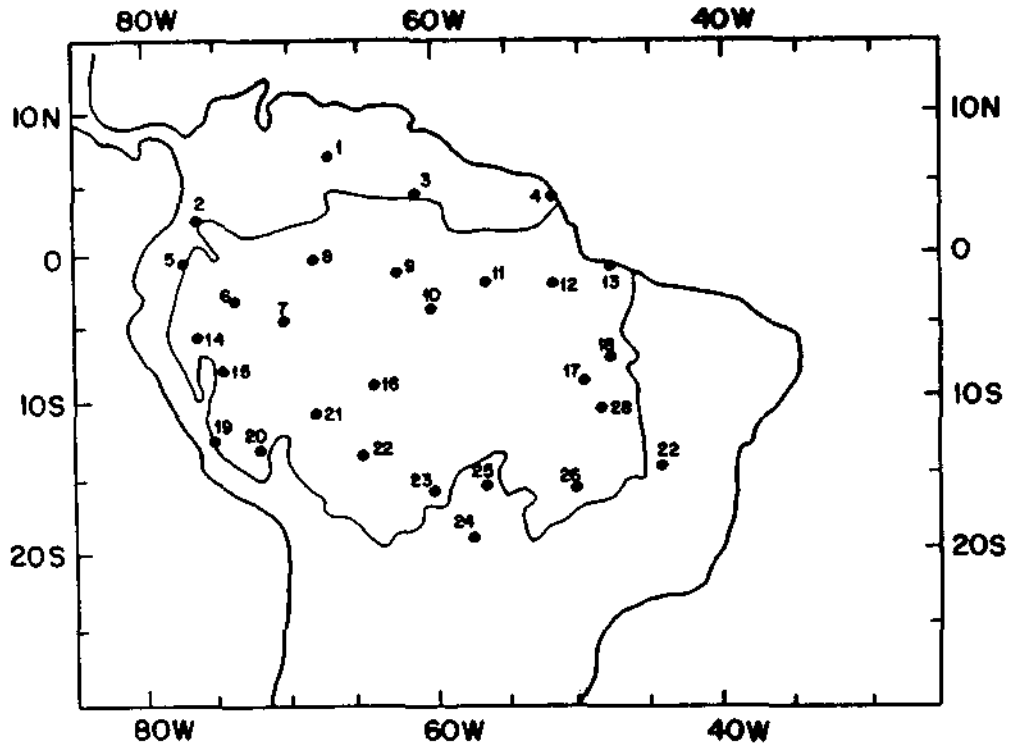

Fig. 1 - Study area and location of stations. The limits of the Amazon River Basin are indicated.

analysis) to describe the dominant spatial modes [25]. Thus the above PCA model takes the form of:

$$Z = FA^{T}$$

where: F(nxm) = Principal component scores
A(mxm) = Principal component loadings

Hence, the principal component loadings were obtained from the input of the correlation matrix R(28x28), which is justified by their advantages which include equal weighting of all the stations to avoid bias positioning of the "synoptic centres" [24].

Table I - The variances (eigenvalues) of the first six unrotated PCs of the precipitation field.

	WITH SEASONAL CYCLE			WITHOUT SEASONAL CYCLE		
PC	VAR.	%	CUM.	VAR.	%	CUM.
1	2.0	42.5	42.5	3.3	11.8	11.8
2	3.6	12.9	55.4	2.2	7.8	19.6
3	1.6	5.5	60.9	1.9	6.9	26.5
4	1.2	4.2	65.1	1.7	6.1	32.6
5	1.0	2.9	68.0	1.4	5.1	37.7
6	0.8	2.6	70.6	1.3	4.6	42.3

The RPC analysis was done in two differents forms: i) with the unaltered time series, and ii)with a time series in which the annual cycle was removed by subtracting the 35-year mean precipitation for each month from the respective monthly value; thus two spatial matrices R(28x28) describing the inter-station correlation were generated. Each matrix was subjected to PCA in order to derive the PCs for these two cases. After obtaining the PCs, by the analysis of their Principal Components Loadings and the variance explained for each eigenvector, we rotated the first six Principal Components in the first case and eight in the second case through the Varimax Method in order to obtain a simple structure of the spatial patterns [25] and to improve their SACZ physical interpretation.

3. RESULTS OF THE ROTATED PRINCIPAL COMPONENT ANALYSIS

The variances (eigenvalues) obtained for both cases are shown in Table I.

In the first case the first four PC's explain 65.1 % of the precipitacion field total variance, whereas on the second case only 32.6 %. This fact can be attributed to the strong seasonal cycle, mainly represented by first PC, in the first case.

a) SERIES WITH SEASONAL CYCLE

In the distribution of the spatial pattern for the first case (Figures 2a-d), areas of maximum and minimum values are well delineated, and their associated time coefficients present strong seasonal cycle (Figures 3a-d); this strong seasonality can be clearly seen in the mean monthly values of the time coefficients (Figures 4a-d). The first spatial pattern (Fig. 2a) shows a marked minimum at the southwestern part of Amazonia with westward penetration; there is also a secondary minimum in the northwest and a maximum in the northern part. The time coefficient series of this pattern (Fig. 3a and 4a) shows positive values in northern summer and negative values in southern summer. This pattern is related to the very well-known dipole type precipitation regime over Amazonia with maximun (minimum) rainfall in the summer (winter) hemisphere. In the southern hemisphere summer the maximum rainfall area [8,22] is due to strong tropical convective activity [11,13,16] associated with the SACZ (South Atlantic Convergence Zone) and generated, in part, by equatorward advance of frontal systems which enhance convective activity [15,28]. Fig. 2b shows the second spatial pattern which presents a strong maximum in northeastern Amazonia over the Amazon river mouth, with a westward tongue-like penetration. The time coefficient series associated to this pattern appears to be related to the annual cycle of the rainfall which would be caused by the seasonal migration of the ITCZ over the Atlantic Ocean near the South American coast [9,27]. The ITCZ reachs its southern most latitude in March-April [27], which suggests that the second pattern may be related to it as the maximum of Fig. 4b occurs also in March-April. Additionally, this pattern appears to be associated to the squall lines [4,7] that form along the Atlantic Coast and propagate inland, where they gradually become less intense in general. The third spatial pattern (Fig. 2c) shows maximum values over the western part of Amazonia and over the Andes, and the time coefficient series (Fig. 3c and 4c) shows maximum values during April and Octobrer and minimum values during January and July. The coefficient series (Fig.3c) resembles the annual march of solar radiation at the Equador which is maximum during the equinoxes and minimun during the solstices. However, this pattern does not lend itself to simple interpretation. Finally the fourth spatial pattern (Fig. 2d) shows a dipole pattern with the Equator aproximately dividing the areas of positive and negative loadings. The time coefficient series (Fig. 3d and 4d) shows positive values in southern hemisphere summer and negative in the other seasons.

b) SERIES WITH ANNUAL CYCLE REMOVED

Figures 5a-d show the spatial patterns of the second case in which the annual cycle was removed. By removing the annual cycle we will be seeking for patterns of interannual variability of rainfall in Amazonia. The first and fourth spatial patterns show simpler structures. The first spatial pattern (Fig. 5a) is similar to the first one of the other case (Fig. 2a). This can be understood by calculating the correlation between the coefficients series for the two cases. The correlation coefficient is 0.65 which shows that the annual cycle was not completely removed and some seasonality still remained. The second spatial patterns (Fig. 5a) shows positive values in southwestern Amazonia and negative values over most of the region. The coefficient time series (Fig. 6b) seems to indicate that rainfall decreased during some ENSO events such as 57/58, 64/65 and 72/73. The third spatial pattern (Fig.5c) shows an area with minimum values in southern Amazonia. The fourth spatial pattern (Fig. 5d) is apparently associated to ENSO events since this spatial distribution agrees well with that of different studies which related ENSO events to precipitation anomalies in Amazonia [1,20]. The time coefficient series (Fig. 6d) shows an example of this relationship for 1982/1983 and 1957/1958.

In order to clarify our understanding of the relationship between ENSO events and the precipitation pattern over the Amazon basin we calculated linear correlations between the SOI time series and the coefficient series for the six RPC of the second case (Table II). In addition cross-spectrum analysis between the same time series was also done.

Table II - Correlation coefficients between the monthly SOI and the first six Rotated Principal Component Scores - RPCS.

RPCS	CORR. COEF.
1	0.08
2	-0.17**
3	-0.02
4	-0.24**
5	0.07
6	-0.09

** significant at 99% confidence level based on null hipotesis of zero correlation

The SOI time series and the coefficient series of the second and fourth pattern are statistically significant at 99% confidence level. Also the coherence-square between the second coefficient series and SOI (Fig.7) shows a peak between 2 and 3 years, statistically significant at 5 % level. This frequency range is one of the dominant frequencies of the ENSO phenomena [5] and it agrees with the frequency range found between the SOI and Amazon River discharges [23]. The coherence-square for the fourth coefficient series (Fig.8) shows a peak at 5 years and is statistically

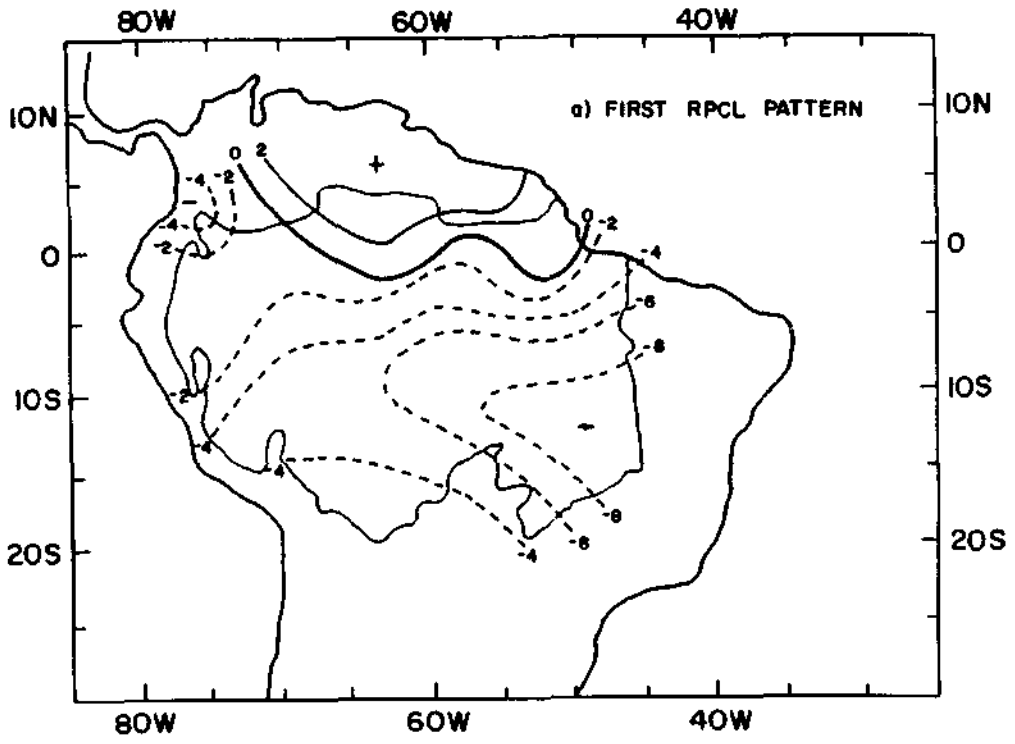

a) First RPCL pattern;

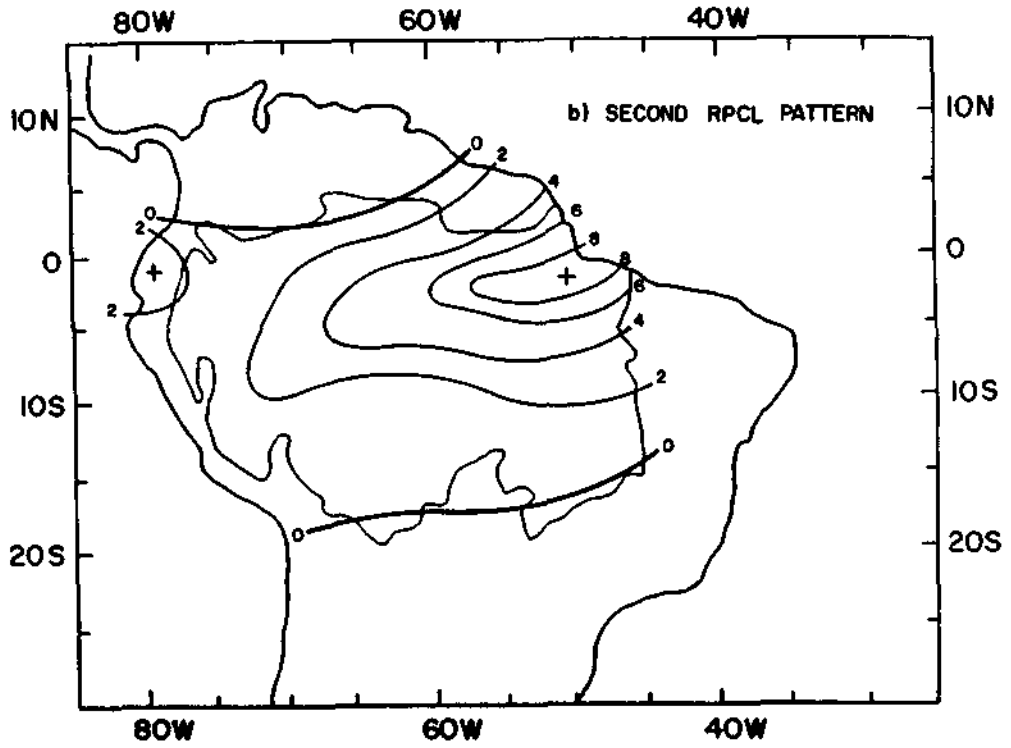

b) Second RPCL pattern;

Fig. 2 - Rotated Principal Component Loading contours (x10) of the first four RPC's of the precipitation field.

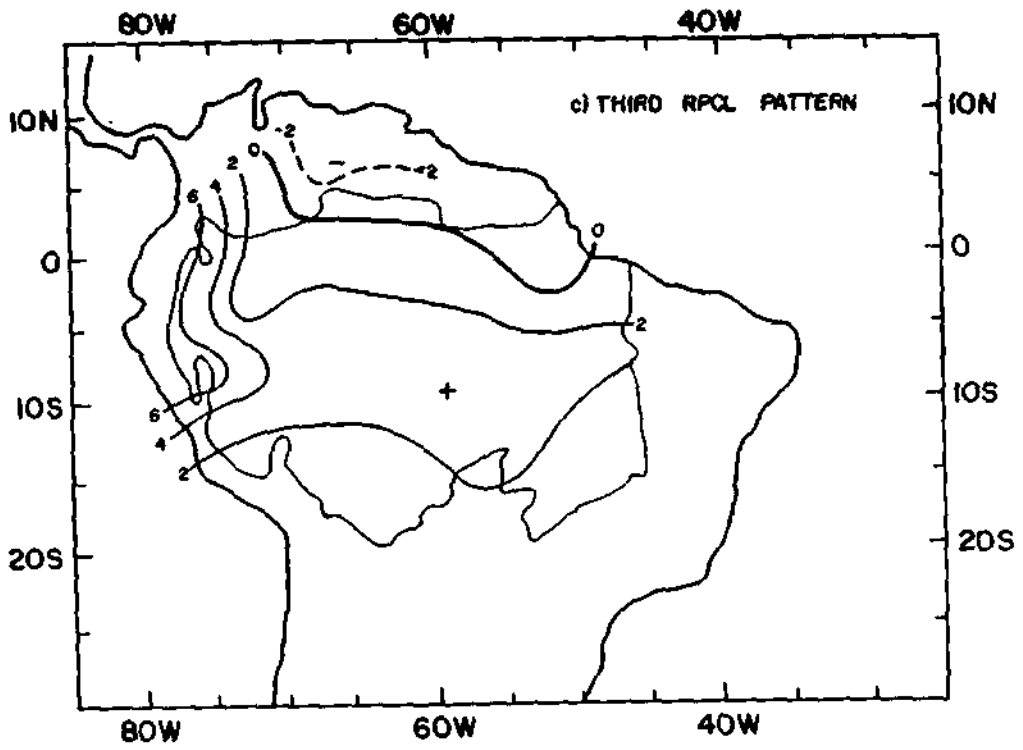

Fig. 2 - c) Third RPCL pattern;

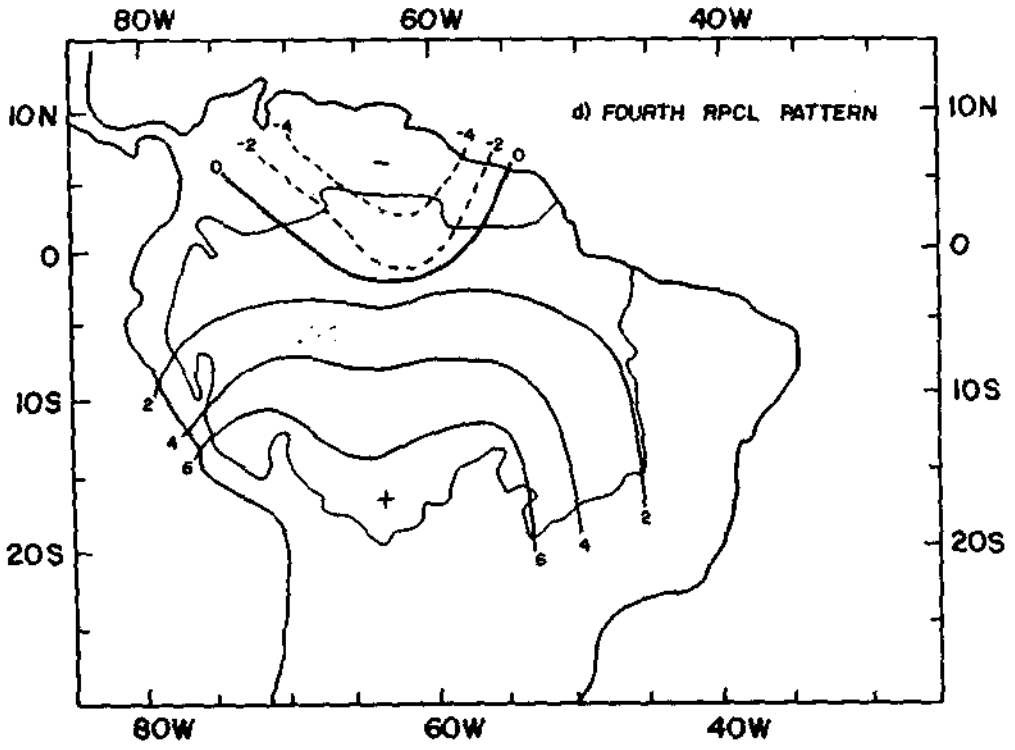

d) Fourth RPCL pattern;

FIG. 2 - Conclusão.

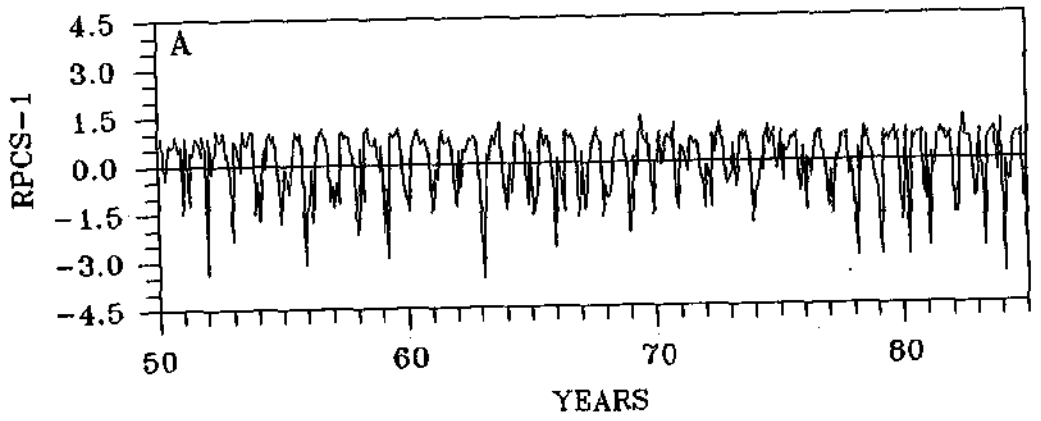

a) First RPCL pattern;

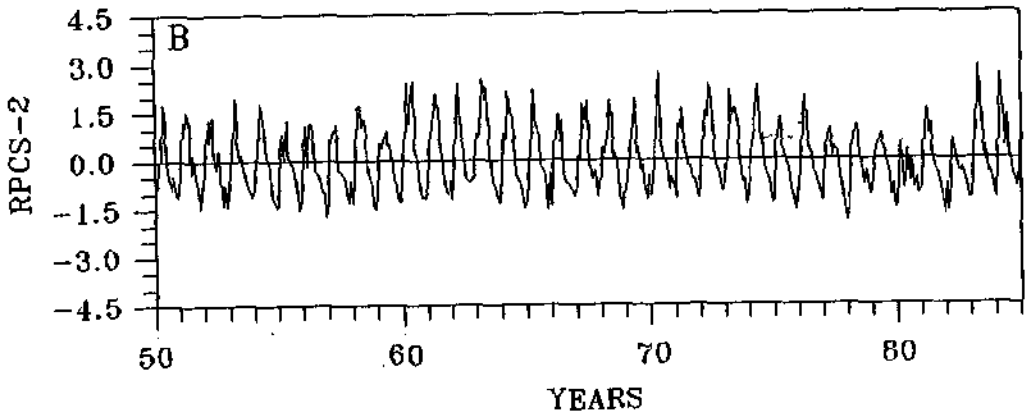

b) Second RPCL pattern;

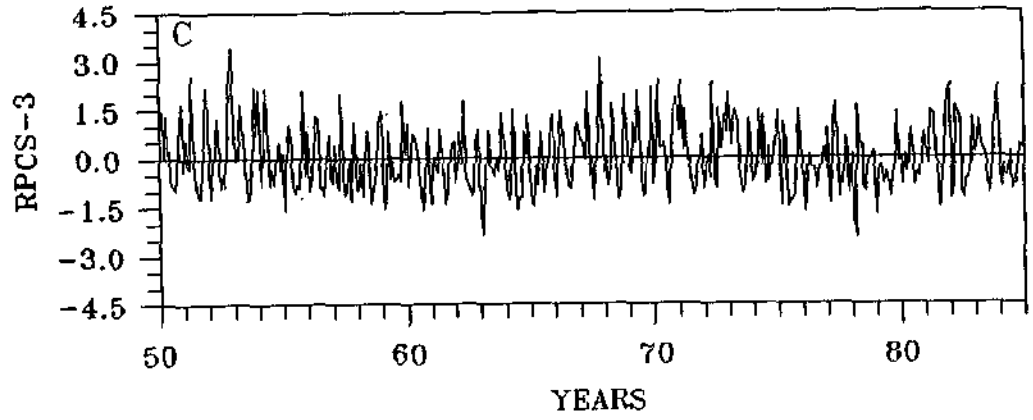

c) Third RPCL pattern;

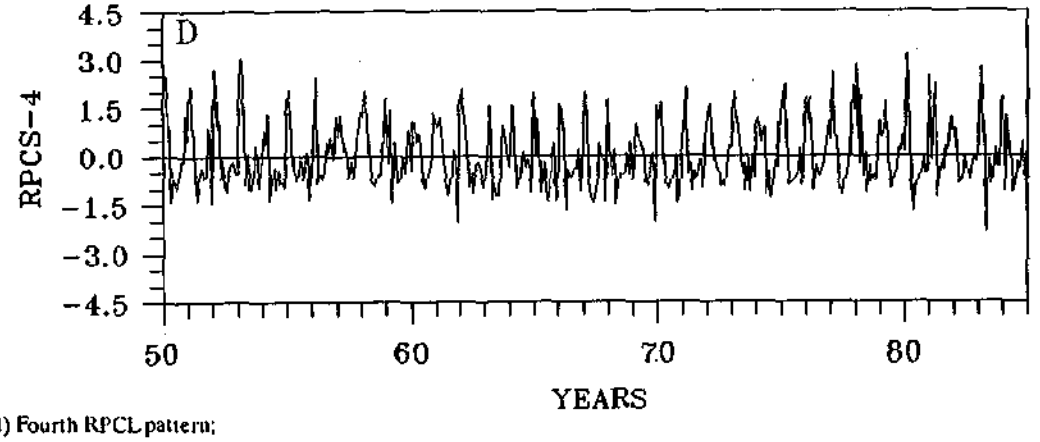

d) Fourth RPCL pattern;

Fig. 3 - RPC Scores of the first four RPC's of the precipitation fields

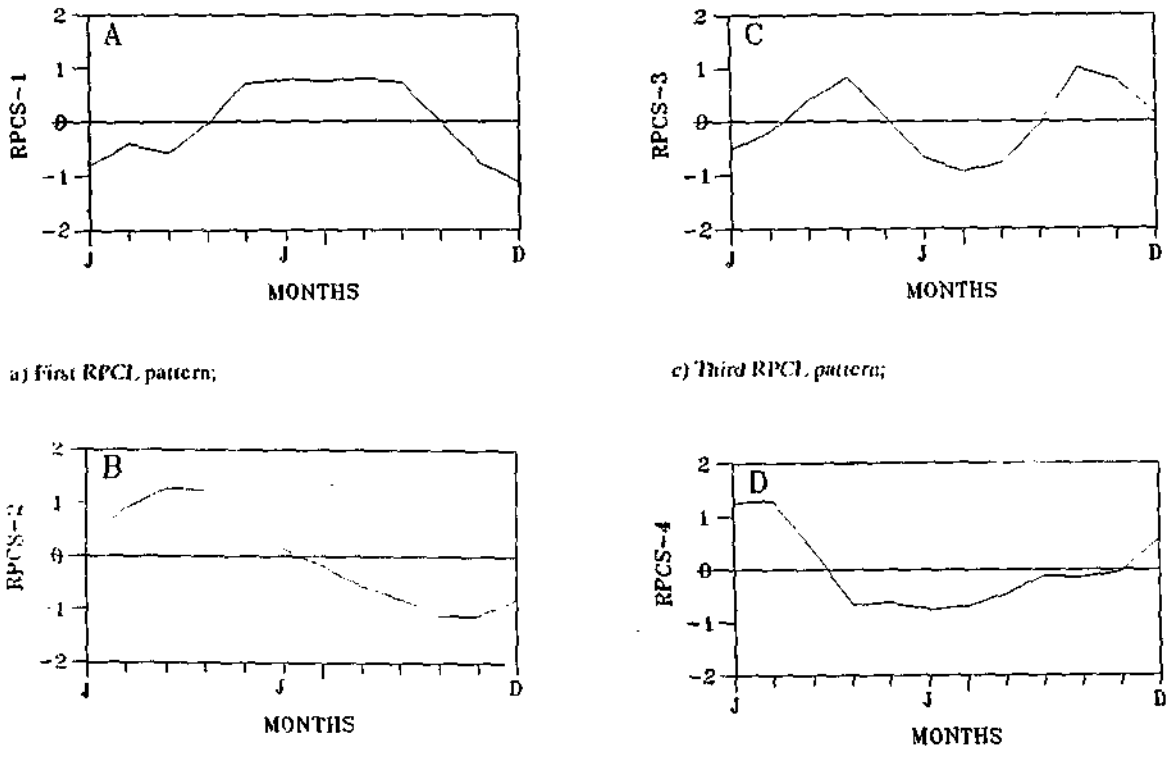

a) First RPCL pattern;

c) Third RPCL pattern;

b) Second RPCL pattern;

d) Fourth RPCL pattern;

Fig. 4 - As in Fig. 3 but for the Monthly mean score of of the first four RPCs of the precipitation field.

significant at 5% level. This spectral peak is also a dominant frequency observed for ENSO phenomena [5,6].

4. CONCLUSIONS

In this study, Rotated Principal Component Analysis (RPCA) was applied to time series of monthly precipitation for 28 stations in the Amazon River Basin. The aim of such analysis was to improve physical understanding of some of the rainfall patterns. The most important findings were the following:

1) With unaltered time series of precipitation (that is, series with annual cycle) two general conclusions can be drawm from the results of this case: i) The first pattern, which explains 42.5% of total variance, is associated with the strong dipole type climatological precipitation over Amazonia with maximum rainfall in the summer hemisphere and minimum rainfall in the winter hemisphere, showing mostly north-south precipitation gradients. The shape of this pattern in the southern Amazonia (NW-SE orientation) seems to indicate its relationship to the seasonal cycle of precipitation associated with the South Atlantic Convergence Zone [15,28]; ii) The second pattern explains 12.9% of total variance and is apparently related to the seasonal cycle of the ITCZ over the Atlantic Ocean and Amazonia's Atlantic Coast [9,18,27]; this pattern also appears to be associated with the squall lines which form along that coast [4,7]. The first two PC's explain 55.5 % of total variance and are strongly linked to the seasonal cycle of precipitation in Amazonia.

2) The annual cycle was removed from the time series to allow easier inspections of possible patterns of interannual variability in Amazonia. A relationship between ENSO events and rainfall over Amazonia seems to exist for the second and fourth patterns of this case. Correlation (Table II) and the cross-spectrum analysis between the SOI time series and the time coefficients series of the two patterns corroborate this finding.

The coefficient series of the second pattern, which is related to ENSO event in the frequency range of 2-3 year, seems to indicate that rainfall decreases during the ENSO events of 57/58, 64/65 and 72/73 but its spatial pattern does not possess a simple interpretation. The fourth pattern of this case, which is related to ENSO events in frequency range of 5 years, appears to be related to ENSO as other observational studies, also have found similar patterns for higher rainfall precipitation anomalies, that is, over northern Peru and Ecuador [10] and deficit precipitation over the eastern part of Amazonia [14,20], during ENSO episodes. This spatial patterns is also found in GCM experiment studies [2].

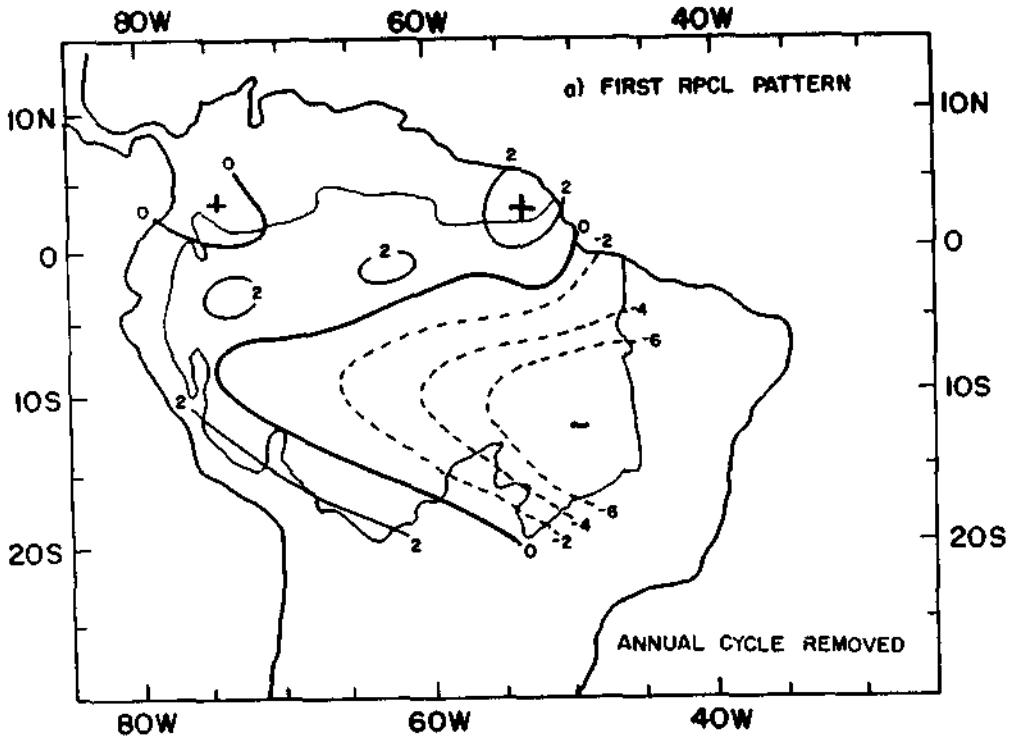

a) first RPCL pattern;

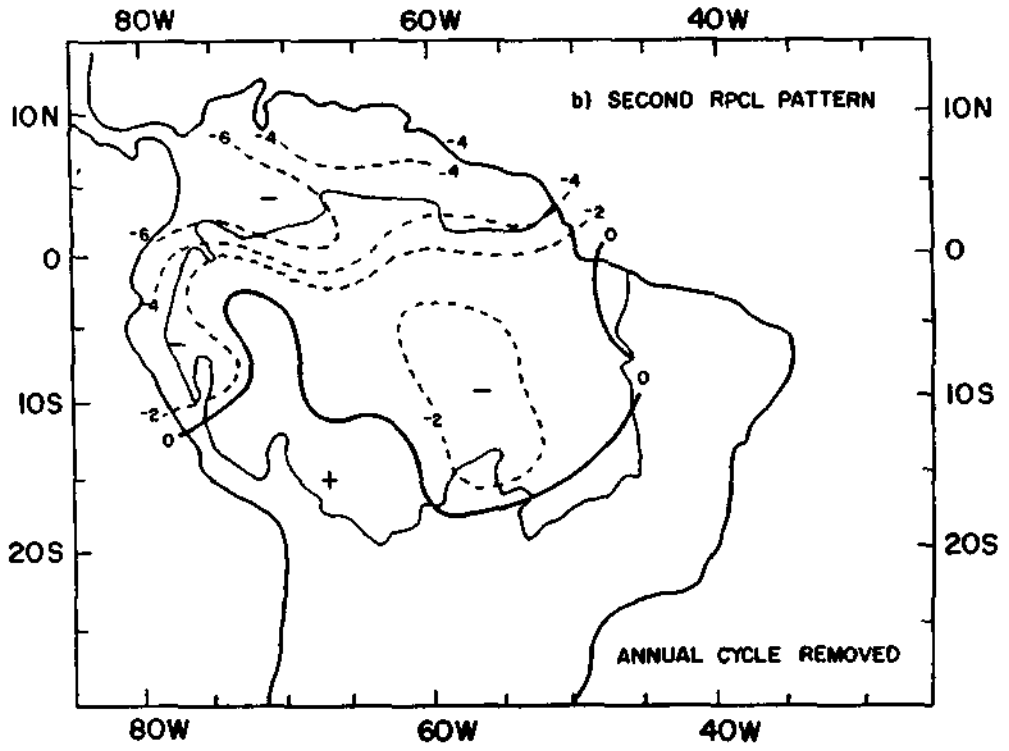

b) Second RPCL pattern;

Fig. 5 - As in Fig. 2 but for precipitation field without the annual cycle.

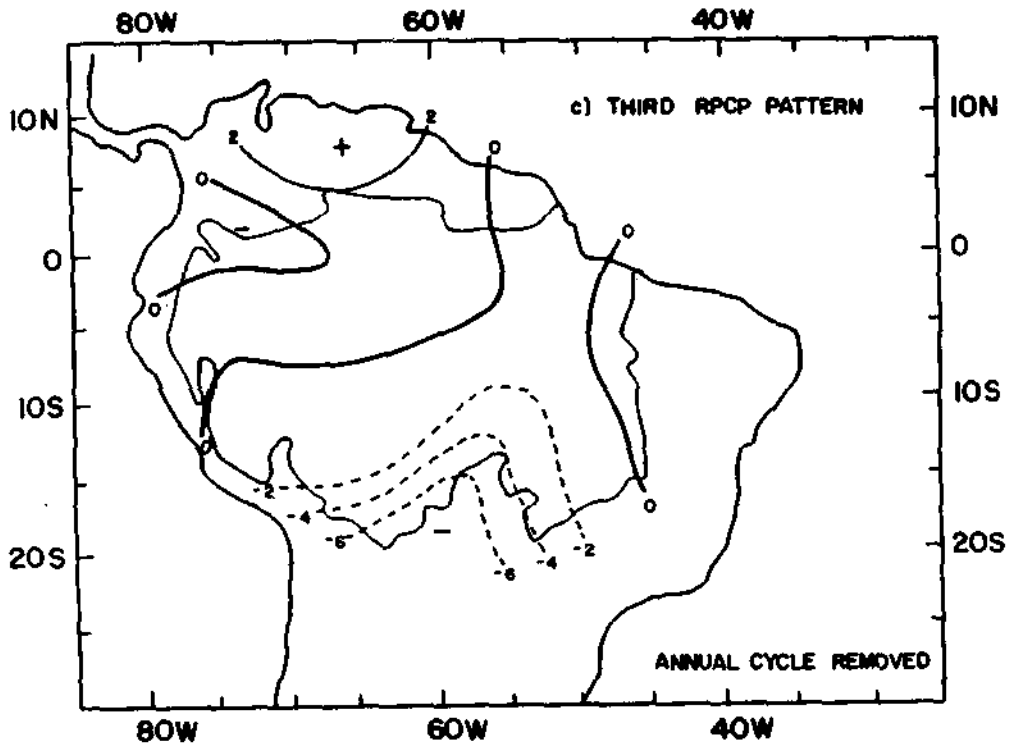

c) Third RPCL pattern;

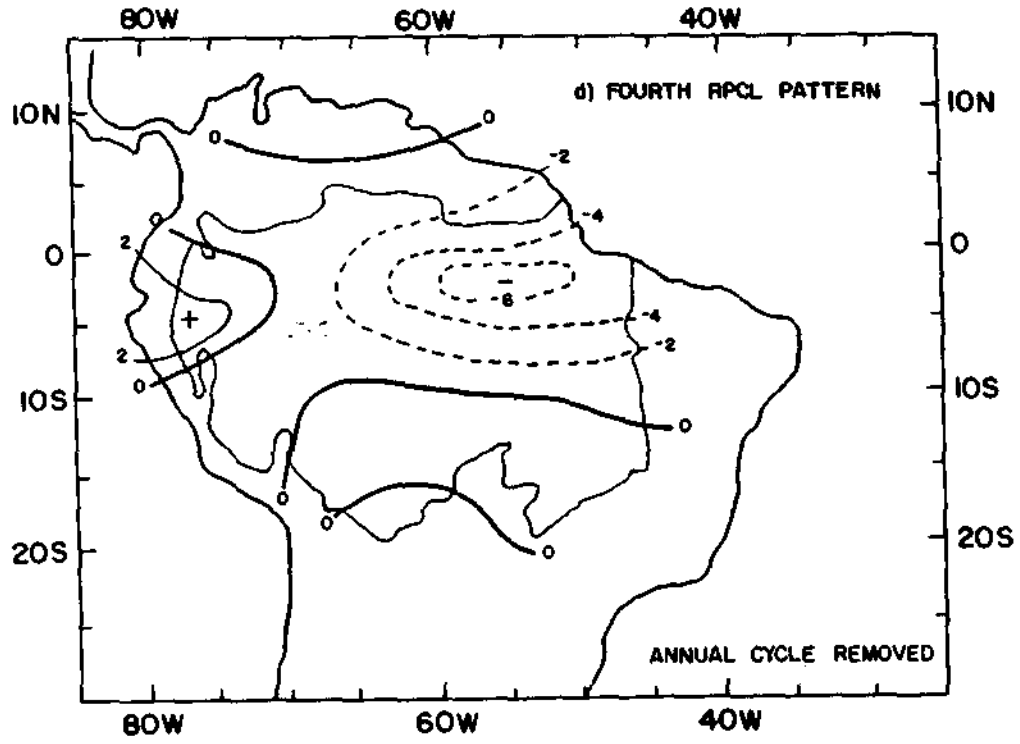

d) Fourth RPCL pattern;

Fig. 5 - Conclusão

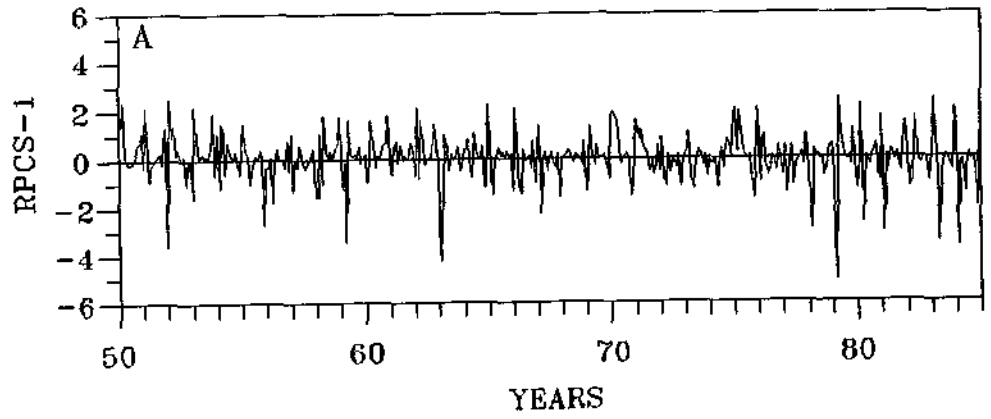

a) First RPCL pattern;

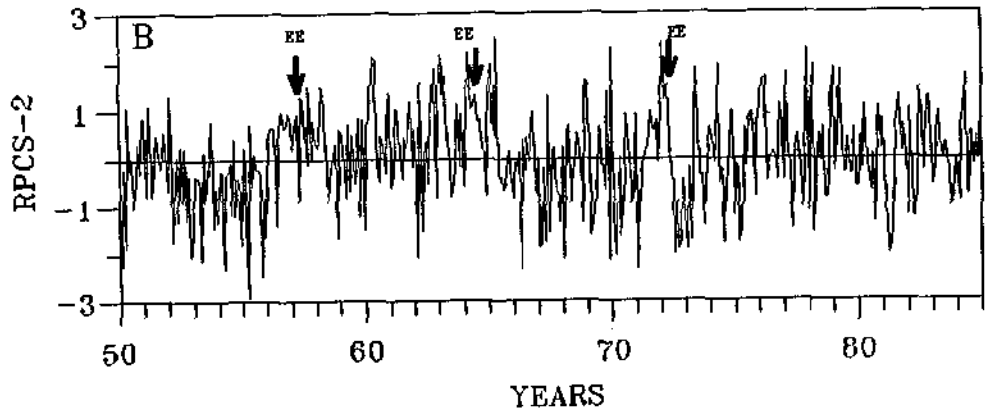

b) Second RPCL pattern;

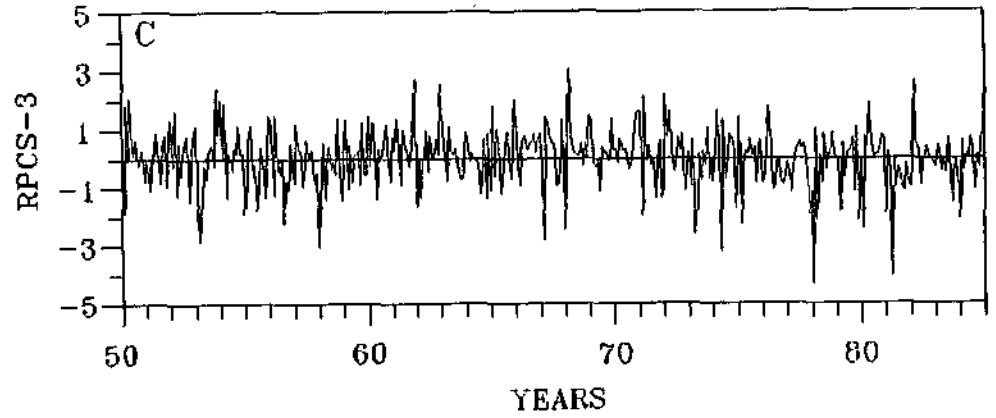

c) Third RPCL pattern;

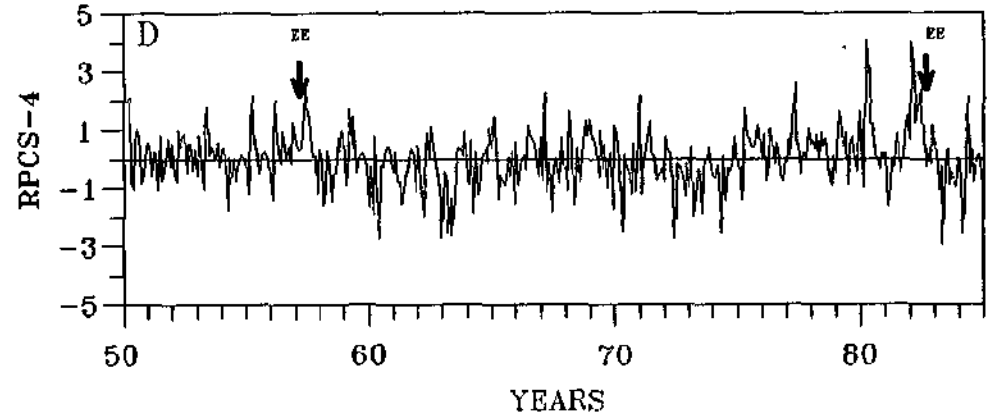

d) Fourth RPCL pattern;

Fig. 6 - As in Fig. 3 but for precipitation field without the annual cycle removed.

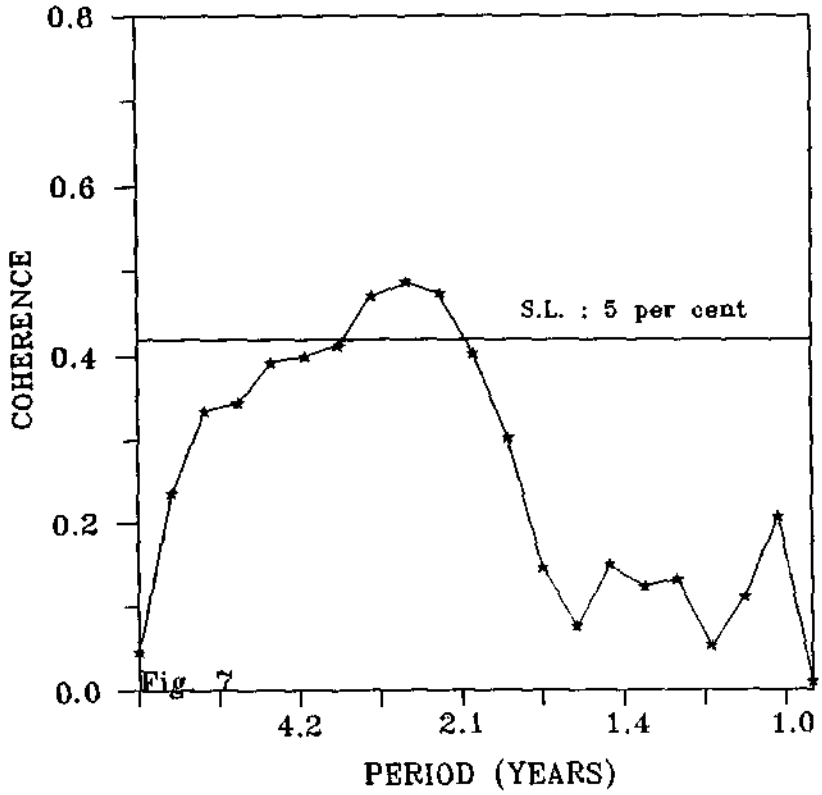

Figure 7 - Coherence square between Southern Oscillation Index (SOI) and RPC Scores of the second pattern without the annual cycle.

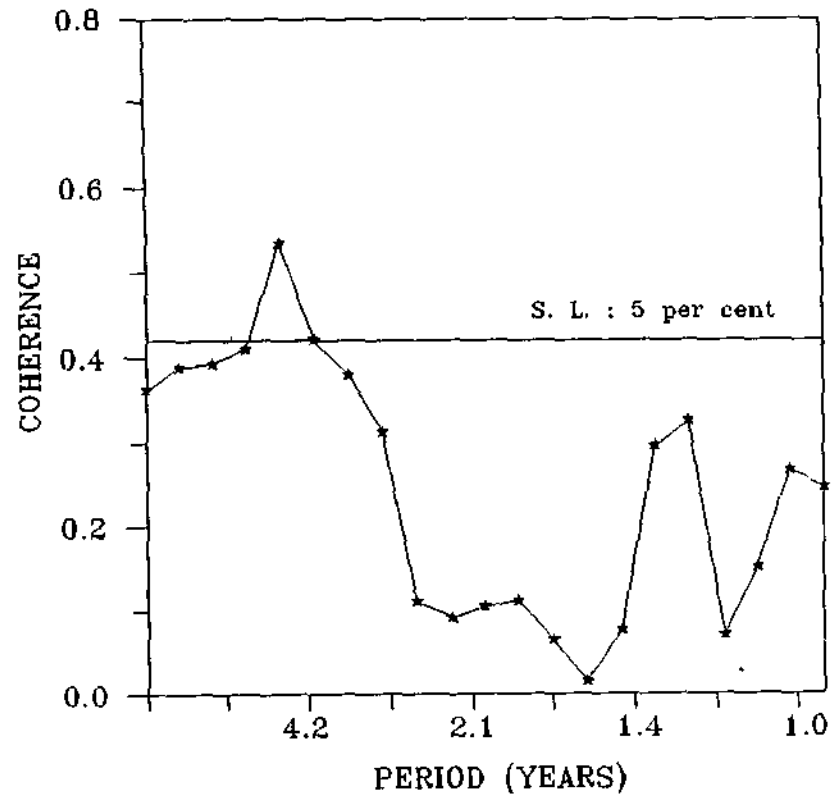

Figure 8 - As in Fig. 7 but for SOI and RPC Scores of the fourth pattern without the annual cycle.

5. ACKNOWLEDGEMENTS

We express our thanks to Paulo Nobre, Ana M. Gusmão and José Ivaldo B. de Brito for providing the corrected precipitation data set for Brazil, to José Marengo and Luis Caceres for providing part of rainfall data sets used in this study and to the Departamento Nacional de Águas e Energia Elétrica (DNAEE) of Brazil.

6. REFERENCES

[1] Aceituno, P., On the functioning of the Southern Oscillation in the South America sector, Mon. Wea.Rev. 116 (1988) 505-524.

[2] Buchman, J., Peagle, J., Buja, L. and Dickinson, R.E., Further FGGE forecast for Amazon Basin Rainfall, Mon.Wea. Rev. 117(1989) 1093-1102.

[3] Caviedes, C., Rainfall in South America. seasonal trends and spatial correlations, Erdkunde 35(1981) 107-118.

[4] Cavalcanti, I.F.A., Um estudo sobre interações entre sistemas de circulações de escala sinótica e circulações locais. Msc. Disertation, (INPE 2494-TDL/097) 1982.

[5] Chen, W.Y., Assessment of southern oscillation sea level pressure indices, Mon.Wea.Rev. 110(1982) 800-807.

[6] Chu, P.S. and Katz, R.W., Spectral estimation from time series models with relevance to Southern Oscillation, J.Climate. 2(1989) 86-90.

[7] Cohen, J.C., Da Silva Dias, M.A.F. and Nobre, C., Aspectos climatológicos das linhas de instabilidade na Amazônia, Climanálise. 4(11) 34-40. 1989.

[8] Figueroa, S.N. and Nobre, C.A., Precipitation distribution over central and western tropical South America, Climanálise. 5(6) 36-4, 1990.

[9] Hastenrath, S. and Heller, L., Dynamics of climatic hazards in Northeast Brazil, Quart.J.Roy Meteor.Soc. 35(1977) 77-92.

[10] Horel, J.D. and Cornejo-Garrido, A.G., Convection along the coast of Norhthern Peru during 1983: Spatial and temporal variation of cloud and rainfall, Mon.Wea.Rev 114(1986) 2091-2105.

[11] Horel, J.D., Hahmann, A.N. and Geisler, J.E., An investigation of convective activity over the Tropical Americas, J.Climate. 1(1989) 1388-1403.

[12] Kayano, M.T., Rao, V.B. and Moura,A.D., The Walker circulation and atmospheric water vapor characteristics over the Pacific for two contrasting years, J.Climatol. 9(1989) 243-252.

[13] Kousky, V.E. and Kagano, M.T., A climatological study of the tropospheric circulation over the Amazon Region, Acta Amazon. 11(1981) 743-758.

[14] Kousky, V.E., Kagano, M.T. and Cavalcanti, I.F.A., A review of the Southern Oscillation: Oceanic-atmospheric circulation changes and related rainfall anomalies, Tellus. 36 A(1984) 490-504.

[15] Kousky, V.E., Atmospheric circulation changes associated with rainfall anomalies over Tropical Brazil, Mon. Wea. Rev. 113 (1985) 1951-1957.

[16] Kousky, V.E., Pentad outgoing longwave radiation climatology for the South America sector, Rev. Bras. de Meteo. 3(1988) 217-231.

[17] Molion, L.C.B., Climatologia dinâmica da região Amazônica: mecanismos de precipição, Rev.Bras. de Meteoro. 2(1987) 107-117.

[18] Moura, A.D. and Shukla, J., On the dynamics of droughts in Northeast Brazil: Observations, theory and numerical expriment with a general General Circulation Model, J. Atmos.Sci. 38(1981) 2653-2675.

[19] Nishizawa, T. and Tanaka, M., The annual changes in the tropospheric circulation and rainfall in South America, Arch.Met.Geoph.Biocl., Ser. B. 33(1983) 107-116.

[20] Nobre, C. and Rennó, N.D., Droughts and floods in South America due to the 1982-83 ENSO episode, in: Proceedings of the 6th Conference on Hurricanes and Tropical Meteorology. AMS., 14-17 May., Houston, Texas, (1985) 131-133.

[21] Oliveira, A.S., Interações entre sistemas frontais na América do Sul e convecção na Amazônia, Tese de Mestrado, INPE-4008-TDL/239. (1986).

[22] Ratisbona, L.R.,The climate of Brazil, in: W. Schwerdtfeger, (eds), Vol. 12. Climates of central and South America(Elsevier, Amsterdam, 1976).

[23] Richey, J.E., Nobre, C. and Deser, C. Amazon river discharge and climatic variability: 1903 to 1985, Science. 246(1989) 101-103.

[24] Richman, M.B., Obliqued rotated Principal Components, An improved meteorological map typing technique?, J.Appl.Meteorol. 20(1981) 1145-1159.

[25] Richman, M.B., Rotation of Principal Components, J.Climatol. 6(1986) 293-335.

[26] Santos, L. do Nacimento, A. and Da Silva, M.G., Um estudo da precipitação da região Amazônica Brasileira usando autovetores empíricos, in: Anais do V Congreso Brasileiro de Meteorologia, Rio de Janeiro (Janeiro 7-Novembro 11 1988).

[27] Uvo, C.R.B., Zona de Convergência intertropical(ZCIT) e sua relação com a precipitação da região Norte e Nordeste Brasil. MSc. Disertation., INPE 4887-TDL/378, (1989).

[28] Virji, H. and Kousky, V.E. Regional and global aspects of the low latitude frontal penetration in Amazonas and associated tropical activity, in: Preprints of the First International Conf. of Southrn Hemisphere Meteology, AMS. São José dos Campos-Brasil (July 31-August 6 1983).

CONTRIBUIÇÕES REPRODUZIDAS NA ÍNTEGRA

PRINCIPAL COMPONENT ANALYSIS OF PRECIPITATION FIELDS OVER THE AMAZON RIVER BASIN

Guillermo O. Obregon and Carlos A. Nobre

Centro de Previsão de Tempo e Estudos Climáticos - CPTEC.
Instituto de Pesquisas Espaciais-INPE
12201 São José dos Campos, SP, Brasil.

ABSTRACT

Rotated Principal Component Analysis (RPCA) was applied to time series of monthly precipitation for 28 stations of Amazon River Basin aiming at improving understanding of some of the spatial rainfall patterns. The precipitation series spanned 35 years(1951-1985). RPCA was performed for both the original series and also for the series which resulted after removal of the annual cycle from the original series. This was done in order to seek for patterns of interannual variability. The first four PC's explain 65.1 % (32.6 %) of total variance for the case with(without) the annual cycle. The first and second patterns of the case with the annual cycle are related to aspects of the seasonal cycle of precipitation over Amazonia: the north-south dipole of maximum precipitation in the summer hemisphere for the first pattern, and the ITCZ seasonal migrations (and related squall lines) along Amazonia's Atlantic Coast for the second. The shape of the first pattern in southern Amazonia suggests its association to the seasonal cycle of the South Atlantic Convergence Zone. The second and fourth patterns of the case without the annual cycle seem to be related to El Nino-South Oscillation (ENSO) events, which is corroborated by cross-spectrum analysis of the Southern Oscillation Index and the time series of the RPC Scores for those two patterns.

RESUMO

Aplicou-se a Análise de Componentes Principais Rotacionadas (ACPR) às séries temporais da precipitação mensal de 28 estações pluviométricas da Bacia Amazônica com vistas a aumentar o entendimento de alguns dos padrões espaciais dos campos de precipitação. As séries de precipitação cobrem o período de 35 anos (1951-1985). Efetuou-se ACPR para as séries originais e, também, para séries onde removeu-se o ciclo anual de modo a procurar-se os padrões de variabilidade interanual dos campos de precipitação. Os quatro primeiros Componentes Principais (CP's) explicam 65.1% (32.6 %) da variância para os casos com o ciclo (sem o ciclo) anual. Os dois primeiros padrões no caso com o ciclo anual relacionam-se fortemente à aspectos do ciclo sazonal de precipitação na Amazônia: o dipólo norte-sul de máximas precipitações no hemisfério de verão para o primeiro padrão, e a migração sazonal da ZCIT (e linhas de instabilidade associadas) na costa atlântica amazônica para o segundo padrão. A forma do primeiro padrão no sul da Amazônia segere uma associação deste com o ciclo sazonal da Zona de Convergência do Atlântico Sul (ZCAS). O segundo e quarto padrões do caso o sem ciclo annual parecem estar relarcionados a eventos El Nino-Oscilação Sul. Verificou-se esta associação através da análise espectral cruzada entre o Índice de Oscilação Sul e os coeficientes das séries temporais (Scores) associados a estes padrões.

1. INTRODUCTION

The region of study is located within latitudes 5°N and 19°S, and longitudes 45°W and 78°W, which approximately marks the limits of the Amazon Basin and lies within the tropical zone of South America. Spatial and temporal variability of rainfall (in this zone [3,8]) is large with strong seasonality. The nature of the precipitation distribution over the Amazon Basin has been investigated [15,19] and reviewed recently [17].

Traditionally, the rainfall climate of Amazonia has been mainly characterized by simple statistes based on monthly or annual totals [3,22]. Recently the climatological precipitation pattern was studied with the aid of EOF's [26]. In this study we used Rotated Principal Component Analysis (RPCA) to study the spatial and temporal variability of the monthly rainfall distribution in Amazonia.

2. DATA AND ANALYSIS METHODS

The data used in this study are the 35 year long (1951-1985) monthly rainfall records of 28 meteorological stations well distributed over the Amazon Basin, as shown in Figure 1. The time series lenght is 420 (35 years x 12 months) for each station. Additionally monthly values of the Southern Oscillation Index (SOI, mean monthly sea level pressure (SLP) anomaly at Darwin minus mean monthly SLP anomaly at Tahity) were used to construct a time series which was correlated to the time series of coefficients of the first 4 RPC's patterns of the precipitation distribution.

The basic principles of PCA are derived from the concept of dispersion of the inicial data matrix Z(nxm); where n = 420 is the length of the monthly precipitation time series and m = 28 the number of stations. The analysis is performed in the space domain (S mode

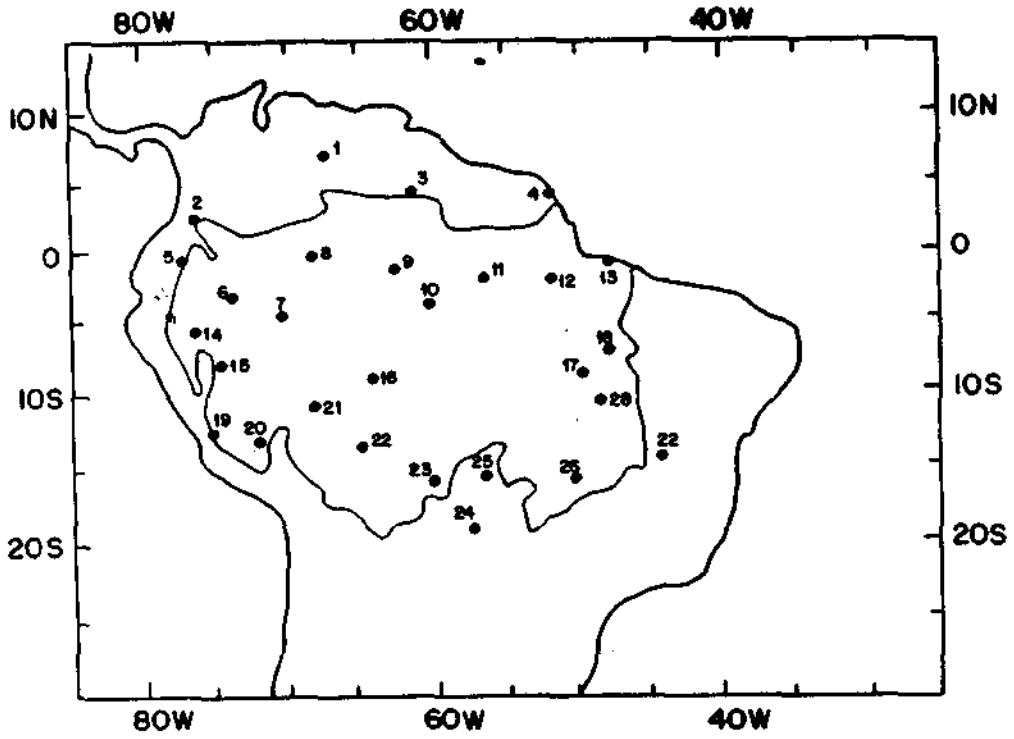

Fig. 1 - Study area and location of stations. The limits of the Amazon River Basin are indicated.

analysis) to describe the dominant spatial modes [25]. Thus the above PCA model takes the form of:

$$Z = FA^T$$

where: F(nxm) = Principal component scores
A(mxm) = Principal component loadings

Hence, the principal component loadings were obtained from the input of the correlation matrix R(28x28), which is justified by their advantages which include equal weighting of all the stations to avoid bias positioning of the "synoptic centres" [24].

Table 1 - The variances (eigenvalues) of the first six unrotated PCs of the precipitation field.

	WITH SEASONAL CYCLE			WITHOUT SEASONAL CYCLE		
PC	VAR.	%	CUM.	VAR.	%	CUM.
1	2.0	42.5	42.5	3.3	11.8	11.8
2	3.6	12.9	55.4	2.2	7.8	19.6
3	1.6	5.5	60.9	1.9	6.9	26.5
4	1.2	4.2	65.1	1.7	6.1	32.6
5	1.0	2.9	68.0	1.4	5.1	37.7
6	0.8	2.6	70.6	1.3	4.6	42.3

The RPC analysis was done in two differents forms: i) with the unaltered time series, and ii)with a time series in which the annual cycle was removed by subtracting the 35-year mean precipitation for each month from the respective monthly value; thus two spatial matrices R(28x28) describing the inter-station correlation were generated. Each matrix was subjected to PCA in order to derive the PCs for these two cases. After obtaining the PCs, by the analysis of their Principal Components Loadings and the variance explained for each eigenvector, we rotated the first six Principal Components in the first case and eight in the second case through the Varimax Method in order to obtain a simple structure of the spatial patterns [25] and to improve their SACZ physical interpretation.

3. RESULTS OF THE ROTATED PRINCIPAL COMPONENT ANALYSIS

The variances (eigenvalues) obtained for both cases are shown in Table I.

In the first case the first four PC's explain 65.1 % of the precipitacion field total variance, whereas on the second case only 32.6 %. This fact can be attributed to the strong seasonal cycle, mainly represented by first PC, in the first case.

a) SERIES WITH SEASONAL CYCLE

In the distribution of the spatial pattern for the first case (Figures 2a-d), areas of maximum and minimum values are well delineated, and their associated time coefficients present strong seasonal cycle (Figures 3a-d); this strong seasonality can be clearly seen in the mean monthly values of the time coefficients (Figures 4a-d). The first spatial pattern (Fig. 2a) shows a marked minimum at the southwestern part of Amazonia with westward penetration; there is also a secondary minimum in the northwest and a maximum in the northern part. The time coefficient series of this pattern (Fig. 3a and 4a) shows positive values in northern summer and negative values in southern summer. This pattern is related to the very well-known dipole type precipitation regime over Amazonia with maximun (minimum) rainfall in the summer (winter) hemisphere. In the southern hemisphere summer the maximum rainfall area [8,22] is due to strong tropical convective activity [11,13,16] associated with the SACZ (South Atlantic Convergence Zone) and generated, in part, by equatorward advance of frontal systems which enhance convective activity [15,28]. Fig. 2b shows the second spatial pattern which presents a strong maximum in northeastern Amazonia over the Amazon river mouth, with a westward tongue-like penetration. The time coefficient series associated to this pattern appears to be related to the annual cycle of the rainfall which would be caused by the seasonal migration of the ITCZ over the Atlantic Ocean near the South American coast [9,27]. The ITCZ reachs its southern most latitude in March-April [27], which suggests that the second pattern may be related to it as the maximum of Fig. 4b occurs also in March-April. Additionally, this pattern appears to be associated to the squall lines [4,7] that form along the Atlantic Coast and propagate inland, where they gradually become less intense in general. The third spatial pattern (Fig. 2c) shows maximum values over the western part of Amazonia and over the Andes, and the time coefficient series (Fig. 3c and 4c) shows maximum values during April and Octobrer and minimum values during January and July. The coefficient series (Fig.3c) resembles the annual march of solar radiation at the Equador which is maximum during the equinoxes and minimun during the solstices. However, this pattern does not lend itself to simple interpretation. Finally the fourth spatial pattern (Fig. 2d) shows a dipole pattern with the Equator aproximately dividing the areas of positive and negative loadings. The time coefficient series (Fig. 3d and 4d) shows positive values in southern hemisphere summer and negative in the other seasons.

b) SERIES WITH ANNUAL CYCLE REMOVED

Figures 5a-d show the spatial patterns of the second case in which the annual cycle was removed. By removing the annual cycle we will be seeking for patterns of interannual variability of rainfall in Amazonia. The first and fourth spatial patterns show simpler structures. The first spatial pattern (Fig. 5a) is similar to the first one of the other case (Fig. 2a). This can be understood by calculating the correlation between the coefficients series for the two cases. The correlation coefficient is 0.65 which shows that the annual cycle was not completely removed and some seasonality still remained. The second spatial patterns (Fig. 5a) shows positive values in southwestern Amazonia and negative values over most of the region. The coefficient time series (Fig. 6b) seems to indicate that rainfall decreased during some ENSO events such as 57/58, 64/65 and 72/73. The third spatial pattern (Fig.5c) shows an area with minimum values in southern Amazonia. The fourth spatial pattern (Fig. 5d) is apparently associated to ENSO events since this spatial distribution agrees well with that of different studies which related ENSO events to precipitation anomalies in Amazonia [1,20]. The time coefficient series (Fig. 6d) shows an example of this relationship for 1982/1983 and 1957/1958.

In order to clarify our understanding of the relationship between ENSO events and the precipitation pattern over the Amazon basin we calculated linear correlations between the SOI time series and the coefficient series for the six RPC of the second case (Table II). In addition cross-spectrum analysis between the same time series was also done.

Table II - Correlation coefficients between the monthly SOI and the first six Rotated Principal Component Scores - RPCS.

RPCS	CORR. COEF.
1	0.08
2	-0.17**
3	-0.02
4	-0.24**
5	0.07
6	-0.09

** significant at 99% confidence level based on null hipotesis of zero correlation

The SOI time series and the coefficient series of the second and fourth pattern are statistically significant at 99% confidence level. Also the coherence-square between the second coefficient series and SOI (Fig.7) shows a peak between 2 and 3 years, statistically significant at 5 % level. This frequency range is one of the dominant frequencies of the ENSO phenomena [5] and it agrees with the frequency range found between the SOI and Amazon River discharges [23]. The coherence-square for the fourth coefficient series (Fig.8) shows a peak at 5 years and is statistically

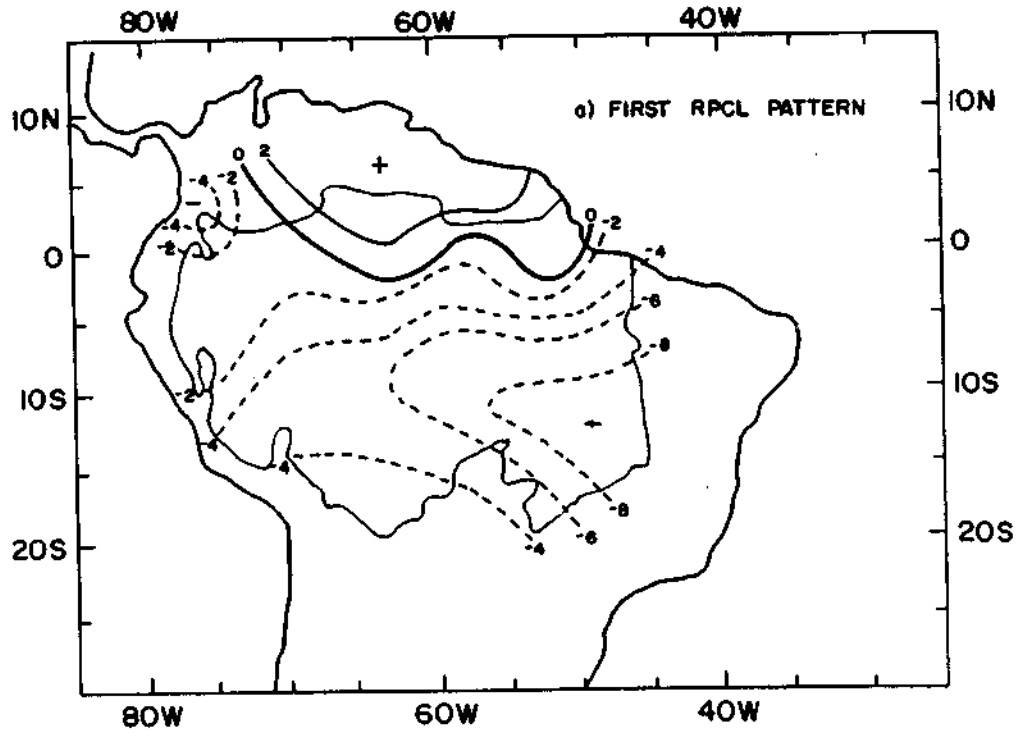

a) First RPCL pattern;

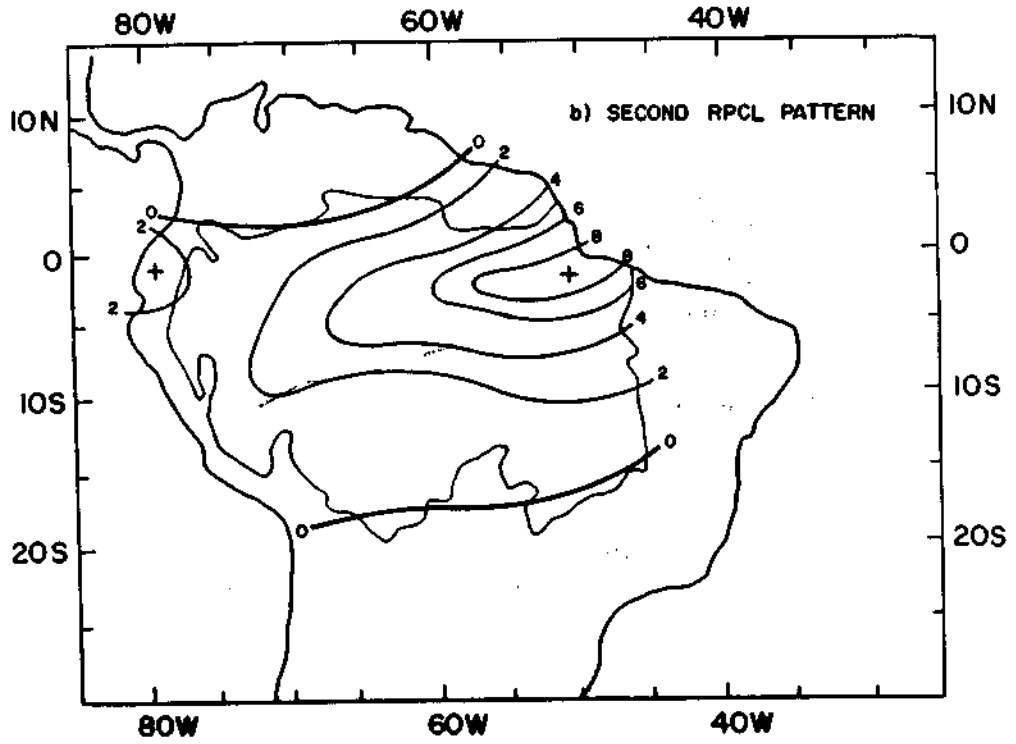

b) Second RPCL pattern;

Fig. 2 - Rotated Principal Component Loading contours (x10) of the first four RPC's of the precipitation field.

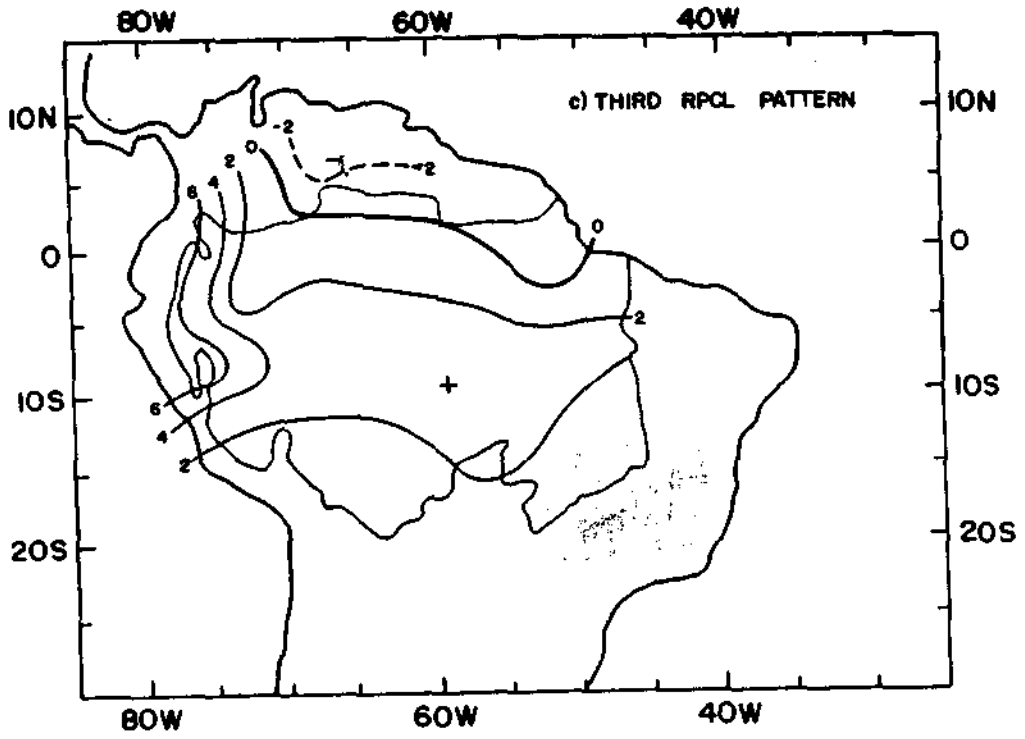

Fig. 2 - c) Third RPCL pattern;

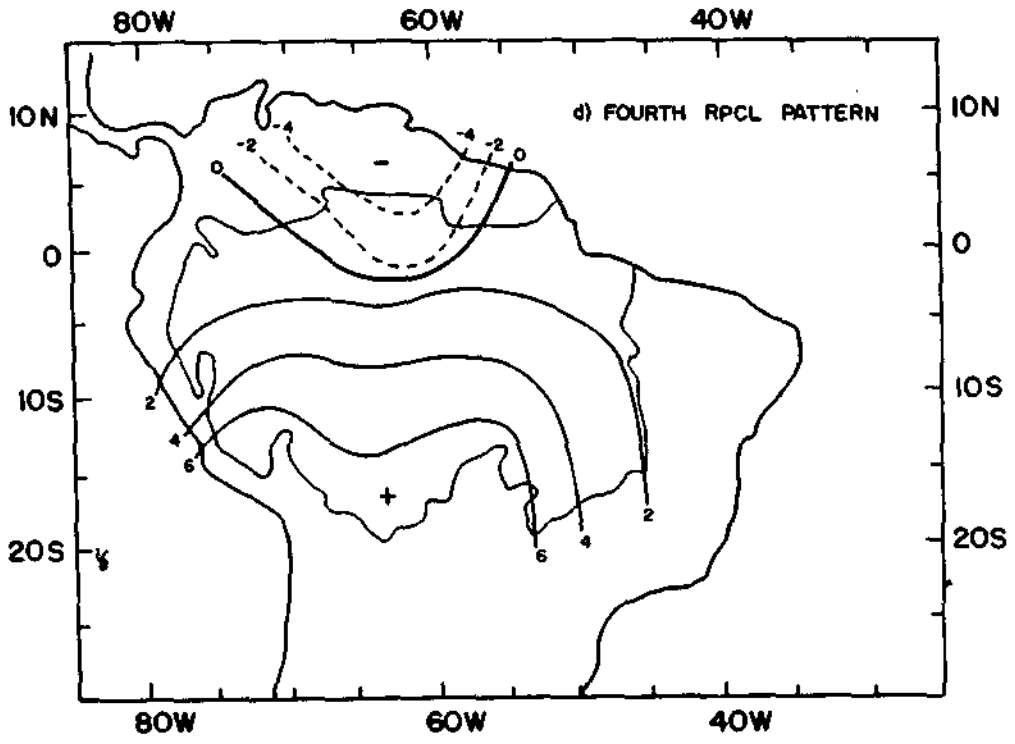

d) Fourth RPCL pattern;

FIG. 2 - Conclusão.

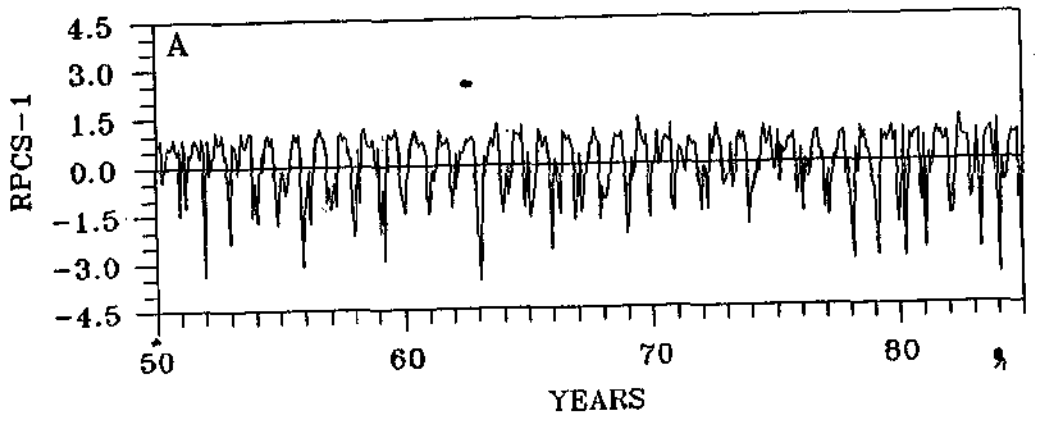

a) First RPCL pattern;

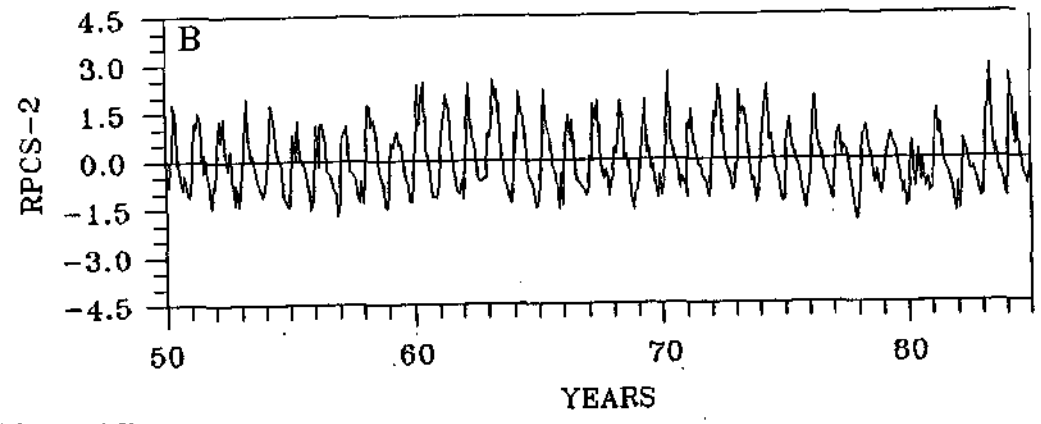

b) Second RPCL pattern;

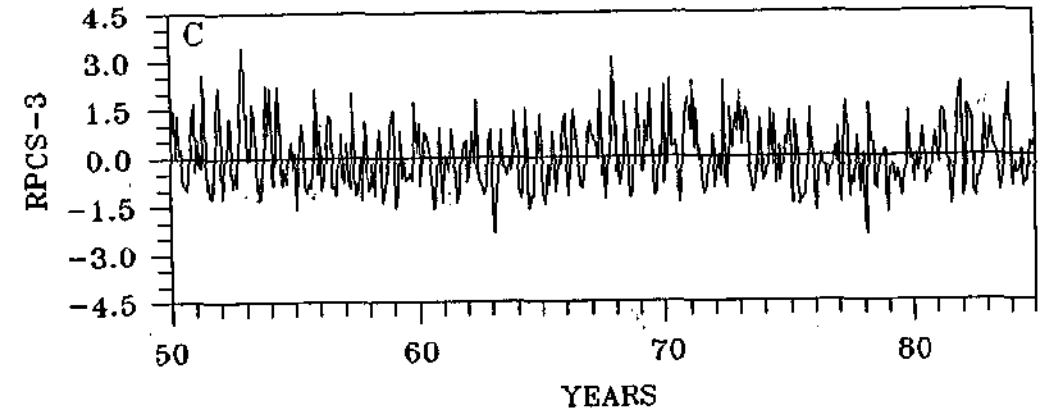

c) Third RPCL pattern;

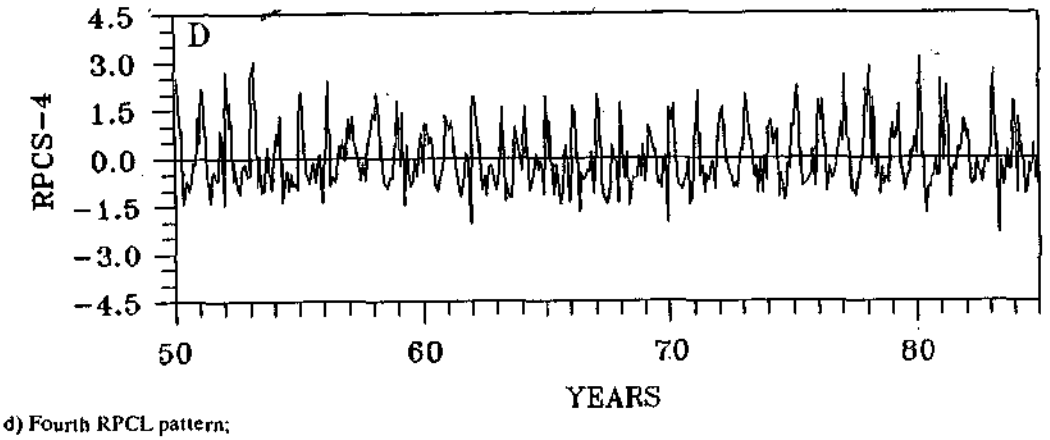

d) Fourth RPCL pattern;

Fig. 3 - RPC Scores of the first four RPC's of the precipitation fields

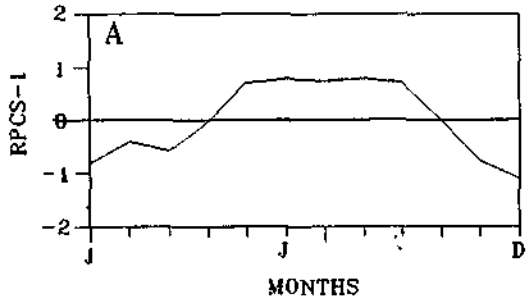

a) First RPCL pattern;

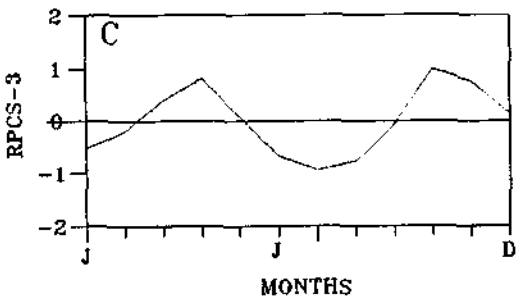

c) Third RPCL pattern;

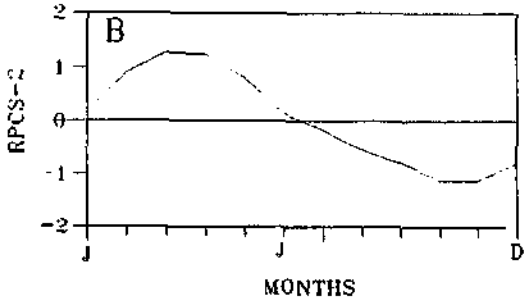

b) Second RPCL pattern;

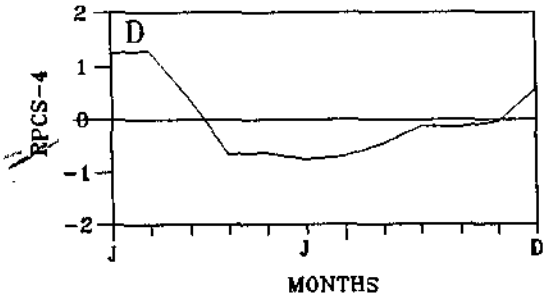

d) Fourth RPCL pattern;

Fig. 4 - As in Fig. 3 but for the Monthly mean score of of the first four RPCs of the precipitation field.

significant at 5% level. This spectral peak is also a dominant frequency observed for ENSO phenomena [5,6].

4. CONCLUSIONS

In this study, Rotated Principal Component Analysis (RPCA) was applied to time series of monthly precipitation for 28 stations in the Amazon River Basin. The aim of such analysis was to improve physical understanding of some of the rainfall patterns. The most important findings were the following:

1) With unaltered time series of precipitation (that is, series with annual cycle) two general conclusions can be drawm from the results of this case: i) The first pattern, which explains 42.5% of total variance, is associated with the strong dipole type climatological precipitation over Amazonia with maximum rainfall in the summer hemisphere and minimum rainfall in the winter hemisphere, showing mostly north-south precipitation gradients. The shape of this pattern in the southern Amazonia (NW-SE orientation) seems to indicate its relationship to the seasonal cycle of precipitation associated with the South Atlantic Convergence Zone [15,28]; ii) The second pattern explains 12.9% of total variance and is apparently related to the seasonal cycle of the ITCZ over the Atlantic Ocean and Amazonia's Atlantic Coast [9,18,27]; this pattern also appears to be associated with the squall lines which form along that coast [4,7]. The first two PC's explain 55.5 % of total variance and are strongly linked to the seasonal cycle of precipitation in Amazonia.

2) The annual cycle was removed from the time series to allow easier inspections of possible patterns of interannual variability in Amazonia. A relationship between ENSO events and rainfall over Amazonia seems to exist for the second and fourth patterns of this case. Correlation (Table II) and the cross-spectrum analysis between the SOI time series and the time coefficients series of the two patterns corroborate this finding.

The coefficient series of the second pattern, which is related to ENSO event in the frequency range of 2-3 year, seems to indicate that rainfall decreases during the ENSO events of 57/58, 64/65 and 72/73 but its spatial pattern does not possess a simple interpretation. The fourth pattern of this case, which is related to ENSO events in frequency range of 5 years, appears to be related to ENSO as other observational studies, also have found similar patterns for higher rainfall precipitation anomalies, that is, over northern Peru and Ecuador [10] and deficit precipitation over the eastern part of Amazonia [14,20], during ENSO episodes. This spatial patterns is also found in GCM experiment studies [2].

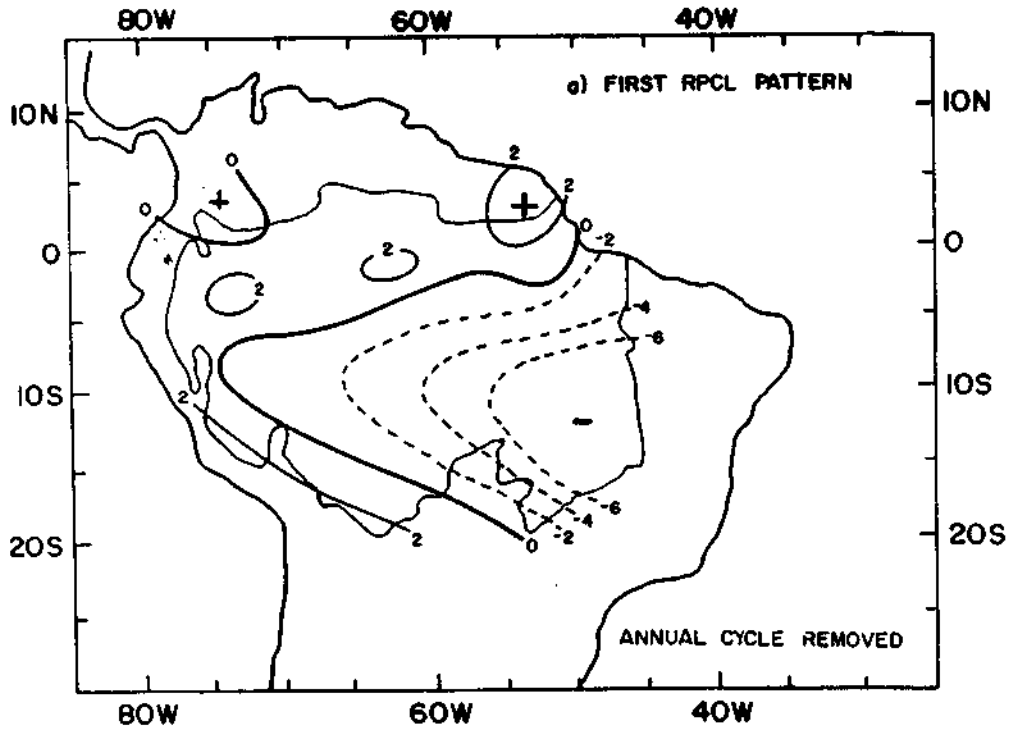

a) first RPCL pattern;

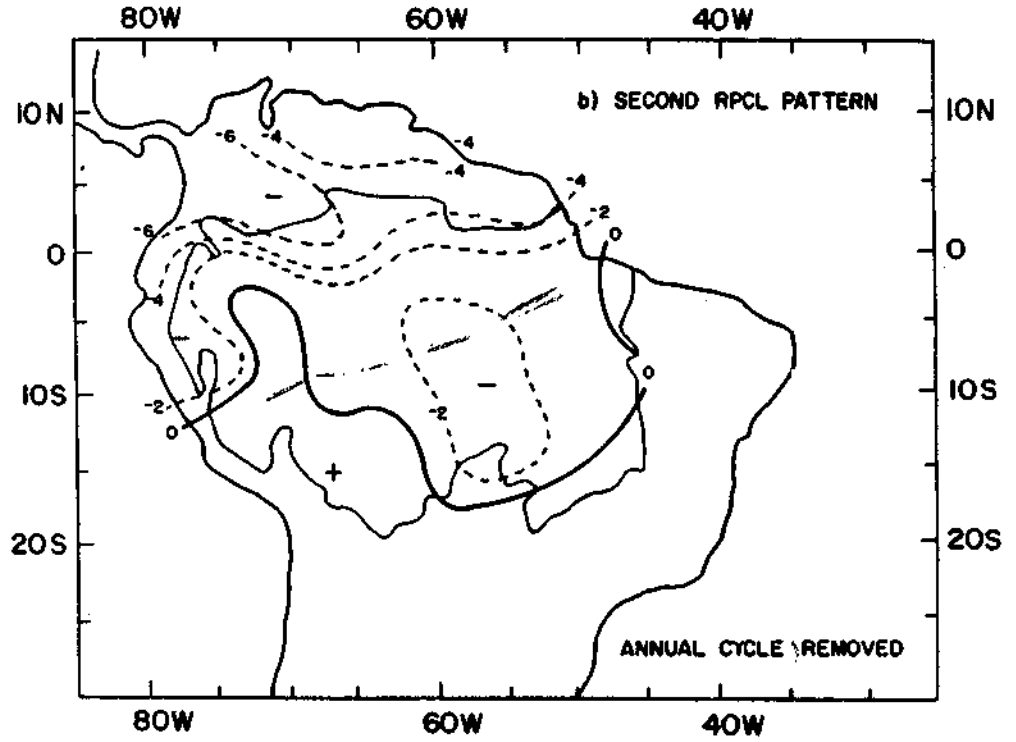

b) Second RPCL pattern;

Fig. 5 - As in Fig. 2 but for precipitation field without the annual cycle.

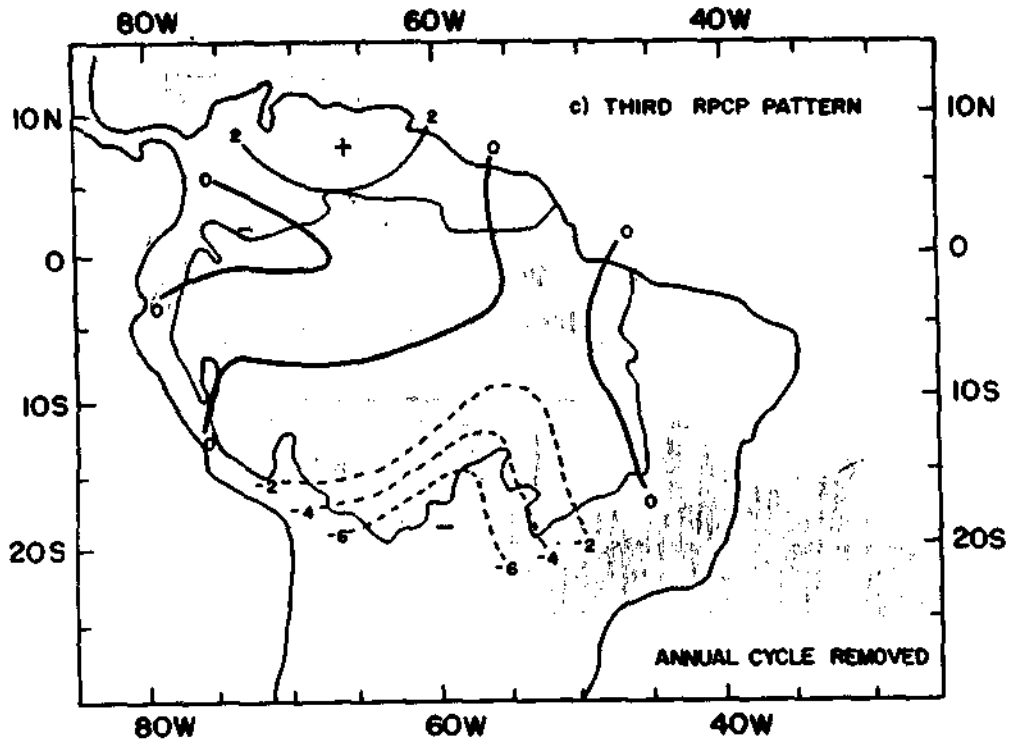

c) Third RPCL pattern;

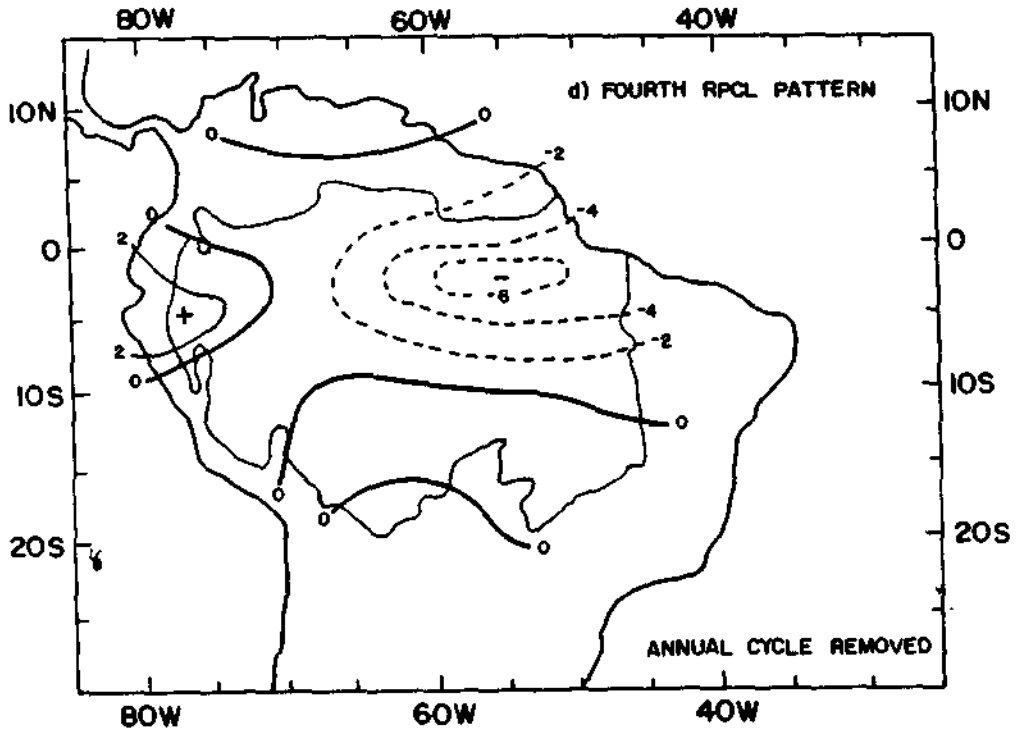

d) Fourth RPCL pattern;

Fig. 5 - Conclusão

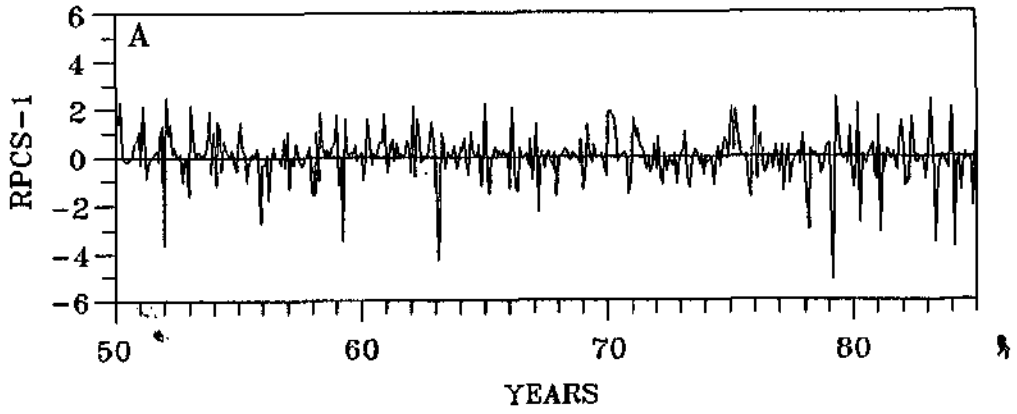

a) First RPCL pattern;

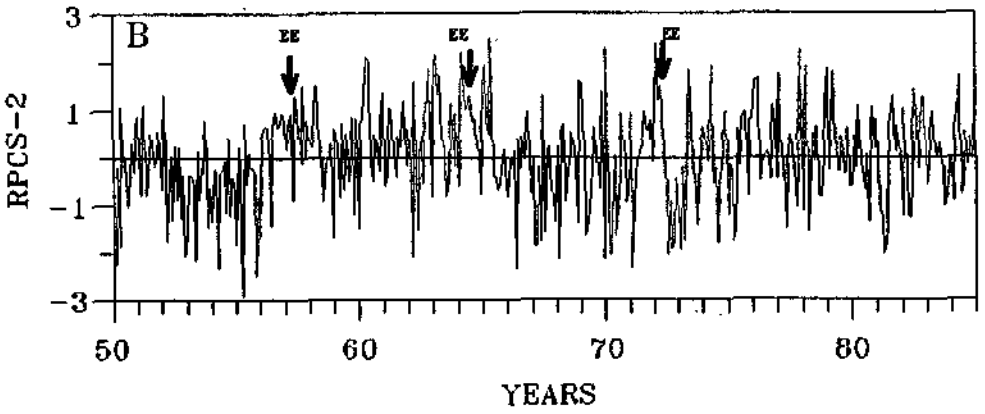

b) Second RPCL pattern;

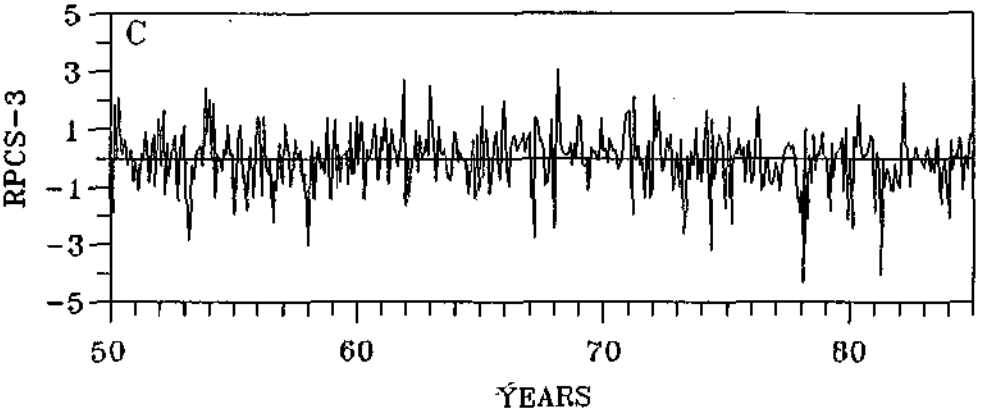

c) Third RPCL pattern;

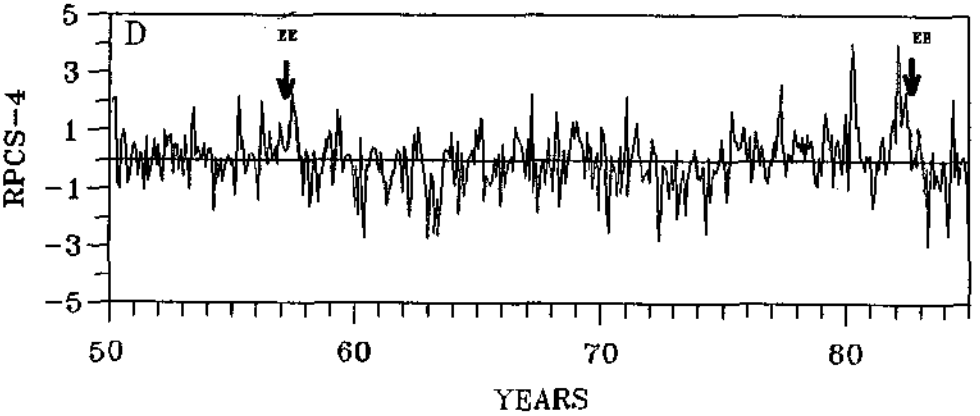

d) Fourth RPCL pattern;

Fig. 6 - As in Fig. 3 but for precipitation field without the annual cycle removed.

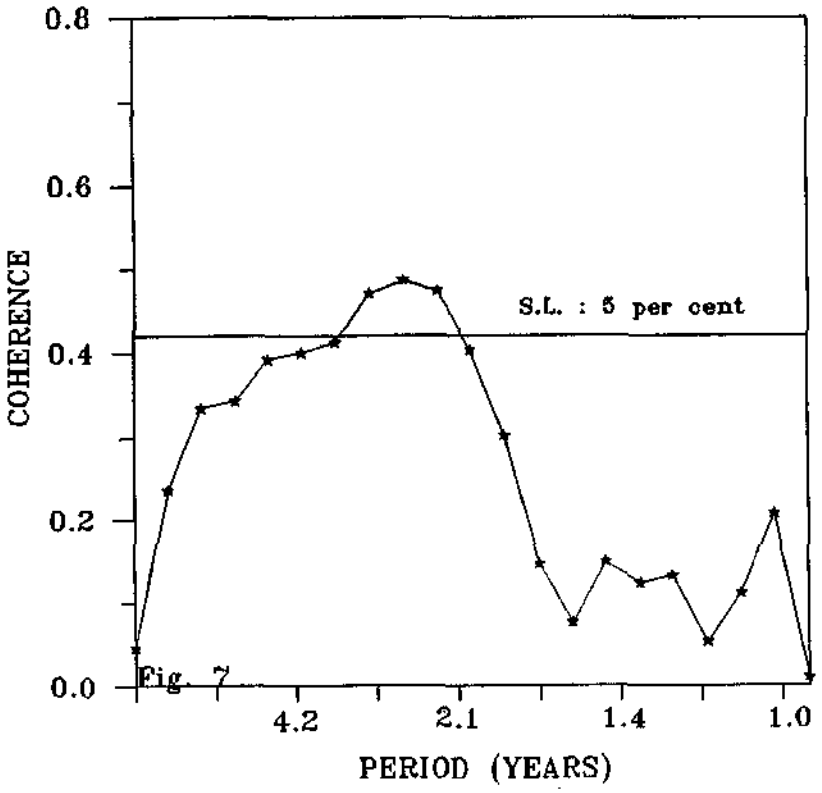

Figure 7 - Coherence square between Southern Oscillation Index (SOI) and RPC Scores of the second pattern without the annual cycle.

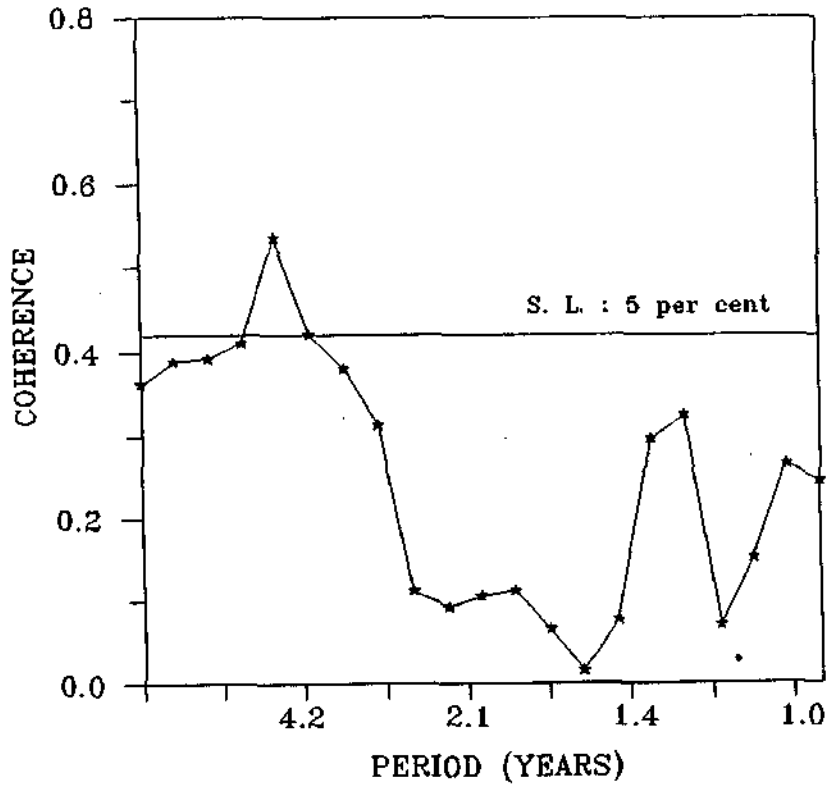

Figure 8 - As in Fig. 7 but for SOI and RPC Scores of the fourth pattern without the annual cycle.

5. ACKNOWLEDGEMENTS

We express our thanks to Paulo Nobre, Ana M. Gusmão and José Ivaldo B. de Brito for providing the corrected precipitation data set for Brazil, to José Marengo and Luis Caceres for providing part of rainfall data sets used in this study and to the Departamento Nacional de Águas e Energia Elétrica (DNAEE) of Brazil.

6. REFERENCES

[1] Aceituno, P., On the functioning of the Southern Oscillation in the South America sector. Mon. Wea.Rev. 116 (1988) 505-524.

[2] Buchman, J., Peagle, J., Buja, L. and Dickinson, R.E., Further PGGE forecast for Amazon Basin Rainfall, Mon.Wea. Rev. 117(1989) 1093-1102.

[3] Caviedes, C., Rainfall in South America, seasonal trends and spatial correlations, Erdkunde 35(1981) 107-118.

[4] Cavalcanti, I.F.A., Um estudo sobre interações entre sistemas de circulações de escala sinótica e circulações locais. Mse. Disertation, (INPE 2494-TDL/097) 1982.

[5] Chen, W.Y., Assessment of southern oscillation sea level pressure indices, Mon.Wea.Rev. 110(1982) 800-807.

[6] Chu, P.S. and Katz, R.W., Spectral estimation from time series models with relevance to Southern Oscillation, J.Climate 2(1989) 86-90.

[7] Cohen, J.C., Da Silva Dias, M.A.F. and Nobre, C., Aspectos climatológicos das linhas de instabilidade na Amazônia. Climanálise, 4(11) 34-40, 1989.

[8] Figueroa, S.N. and Nobre, C.A., Precipitation distribution over central and western tropical South America, Climanálise, 5(6) 36-4, 1990.

[9] Hastenrath, S. and Heller, L., Dynamics of climatic hazards in Northeast Brazil, Quart.J.Roy Meteor.Soc. 35(1977) 77-92.

[10] Horel, J.D. and Cornejo-Garrido, A.G., Convection along the coast of Norththern Peru during 1983: Spatial and temporal variation of cloud and rainfall, Mon.Wea.Rev 114(1986) 2091-2105.

[11] Horel, J.D., Hahmann, A.N. and Geisler, J.E., An investigation of convective activity over the Tropical Americas, J.Climate. 1(1989) 1388-1403.

[12] Kayano, M.T., Rao, V.B. and Moura,A.D., The Walker circulation and atmospheric water vapor characteristics over the Pacific for two contrasting years, J.Climatol. 9(1989) 243-252.

[13] Kousky, V.E. and Kagano, M.L., A climatological study of the tropospheric circulation over the Amazon Region, Acta Amazon. 11(1981) 743-758.

[14] Kousky, V.E., Kagano, M.T. and Cavalcanti, I.F.A., A review of the Southern Oscillation: Oceanic-atmospheric circulation changes and related rainfall anomalies, Tellus, 36 A(1981) 490-504.

[15] Kousky, V.E., Atmospheric circulation changes associated with rainfall anomalies over Tropical Brazil, Mon. Wea. Rev. 113 (1985) 1951-1957.

[16] Kousky, V.E., Pentad outgoing longwave radiation climatology for the South America sector, Rev. Bras. de Meteo. 3(1988) 217-231.

[17] Molion, L.C.B., Climatologia dinâmica da região Amazônica mecanismos de precipição, Rev.Bras. de Meteoro. 2(1987) 107-117.

[18] Moura, A.D. and Shukla, J., On the dynamics of droughts in Northeast Brazil: Observations, theory and numerical expriment with a general General Circulation Model, J Atmos.Sci. 38(1981) 2653-2675.

[19] Nishizawa, T. and Tanaka, M., The annual changes in the tropospheric circulation and rainfall in South America Arch.Met.Geoph.Biocl., Ser. B, 33(1983) 107-116.

[20] Nobre, C. and Rennó, N.D., Droughts and floods in South America due to the 1982-83 ENSO episode, in: Proceedings of the 6th Conference on Hurricanes and Tropical Meteorology, AMS., 14-17 May., Houston, Texas, (1985) 131-133.

[21] Oliveira, A.S., Interações entre sistemas frontais na América do Sul e convecção na Amazônia, Tese de Mestrado INPE-4008-TDL/239, (1986).

[22] Ratisbona, L.R., The climate of Brazil, in: W. Schwerdtfeger (eds), Vol 12, Climates of central and South America(Elsevier Amsterdam, 1976)

[23] Richey, J.E., Nobre, C. and Deser, C., Amazon river discharge and climatic variability: 1903 to 1985, Science, 246(1989) 101-103.

[24] Richman, M.B., Obliqued rotated Principal Components :An improved meteorological map typing technique? J.Appl.Meteorol. 20(1981) 1145-1159.

[25] Richman, M.B., Rotation of Principal Components, J.Climatol 6(1986) 293-335.

[26] Santos, L. do Nacimento, A. and Da Silva, M.G., Um estudo da precipitação da região Amazônica Brasileira usando autovetores empíricos, in: Anais do V Congreso Brasileiro de Meteorologia, Rio de Janeiro (Janeiro 7-Novembro 11 1988)

[27] Uvo, C.R.B., Zona de Convergência intertropical(ZCIT) e sua relação com a precipitação da região Norte e Nordeste Brasil MSc. Dissertation, INPE-4887-TDI/378, (1989).

[28] Virji, H. and Kousky, V.E., Regional and global aspects of the low latitude frontal penetration in Amazonas and associated tropical activity, in: Preprints of the First International Conf. of Southrn Hemisphere Meteology, AMS, São José dos Campos-Brasil (July 31-August 6 1983)